

Optimization-Informed Neural Networks

Dawen Wu^{a,*}, Abdel Lisser^a

^a*Université Paris-Saclay, CNRS, CentraleSupélec, Laboratoire des signaux et systèmes, 91190, Gif-sur-Yvette, France*

Abstract

Solving constrained nonlinear optimization problems (CNLPs) is a longstanding computational problem that arises in various fields, e.g., economics, computer science, and engineering. We propose optimization-informed neural networks (OINN), a deep learning approach to solve CNLPs. By neurodynamic optimization methods, a CNLP is first reformulated as an initial value problem (IVP) involving an ordinary differential equation (ODE) system. A neural network model is then used as an approximate state solution for this IVP, and the endpoint of the approximate state solution is a prediction to the CNLP. We propose a novel training algorithm that directs the model to hold the best prediction during training. In a nutshell, OINN transforms a CNLP into a neural network training problem. By doing so, we can solve CNLPs based on deep learning infrastructure only, without using standard optimization solvers or numerical integration solvers. The effectiveness of the proposed approach is demonstrated through a collection of classical problems, e.g., variational inequalities, nonlinear complementary problems, and standard CNLPs.

Keywords: Constrained nonlinear optimization problems, Neural networks, Neurodynamic optimization, ODE system

1. Introduction

Constrained nonlinear optimization problems (CNLPs) play a central role in operations research and have a wide range of real-world applications, such as production planning, resource allocation, portfolio selection, portfolio optimization, feature selection, equilibrium problems (Xiao & Boyd, 2006; Leung & Wang, 2020; Wang et al., 2021; Wu & Lisser, 2022). CNLPs have been studied at both the theoretical and practical levels for the last few decades (Bertsekas, 1997; Boyd et al., 2004).

Neurodynamic optimization methods model a CNLP by the mean of an ordinary differential equation (ODE) system. Hopfield & Tank (1985) pioneered this study and solved the well-known “traveling salesman” problem by the Hopfield network. Kennedy & Chua (1988) extended the method to solve nonlinear convex programming problems by using a penalty parameter. However, the disadvantage of this penalty parameter method is that the true minimizer is obtained only when the penalty parameter goes to infinity. When the penalty parameter is too large, the method hardly converges to the optimal solution. Since then, researchers

*Corresponding author

Email address: dawen.wu@centralesupelec.fr, abdel.lisser@12s.centralesupelec.fr (Abdel Lisser)

have improved the method gradually without using the penalty parameter. Rodriguez-Vazquez et al. (1990); Xia et al. (2002); Gao et al. (2004); Xia & Feng (2007); Xia & Wang (2015) proposed neurodynamic methods based on a projection function. Besides the convex and smooth optimization problems, Forti et al. (2004); Xue & Bian (2008); Qin & Xue (2014) solved non-smooth CNLPs using differential inclusion theory and sub-gradient. Additionally, pseudoconvex optimization problems have been studied based on various assumptions (Guo et al., 2011; Qin et al., 2013; Xu et al., 2020).

With the rapid growth of available data and computing resources, deep learning now has a wide range of applications, e.g., image processing (Krizhevsky et al., 2012; Goodfellow et al., 2016), natural language processing (Devlin et al., 2018), bioinformatics (Min et al., 2017; Jumper et al., 2021). In operations research, a neural network is used as a solver component to solve the mixed integer programming problem (Nair et al., 2020). Graphical neural networks can be used for combinatorial optimization problems directly as solvers or to enhance standard solvers (Cappart et al., 2021).

Dissanayake & Phan-Thien (1994) initially used a neural network as an approximate solution to differential equations, where the training objective is to satisfy the given differential equation and boundary conditions. Lagaris et al. (1998) constructed a neural network to satisfy an initial/boundary condition, and they discussed the use of ODE and PDE problems, respectively. Lagaris et al. (2000); McFall & Mahan (2009) extended the Lagris' method to irregular boundaries. Raissi et al. (2019) introduced physics-informed neural networks to solve forward and inverse problems involving PDEs. Sirignano & Spiliopoulos (2018) presents a theoretical analysis that shows the neural network approximator converges to the PDE solution as hidden units go to infinity. Deep learning approaches are attempting to overcome the challenge of solving high-dimensional nonlinear PDEs (Han et al., 2017; Yu et al., 2018; Han et al., 2018; Beck et al., 2019). This line of research has been extended to various fields, e.g., computational mechanics (Anitescu et al., 2019; Samaniego et al., 2020; Guo et al., 2021). All the above methods use one neural network to solve one ODE/PDE problem. Flamant et al. (2020) parameterizes ODE systems and uses the parameters as an input to a neural network so that one neural network can solve multiple ODE systems. The universal approximation theorem of neural networks states that a neural network can approximate any continuous function to arbitrary accuracy (Cybenko, 1989; Hornik et al., 1989; Sonoda & Murata, 2017). Automatic differentiation tools facilitate the computation of derivative, gradient, and Jacobian matrix (Baydin et al., 2018; Paszke et al., 2019). Software packages have been developed to implement these deep learning methods for solving differential equations (Lu et al., 2021; Chen et al., 2020).

1.1. Contributions

The contributions of this paper can be summarized as follows.

- We propose a deep learning approach to solve CNLPs, namely OINN. To the best of our knowledge, this is the first time deep learning is used to solve CNLPs. OINN reformulates a CNLP as a neural network training problem via neurodynamic optimization. Thus, we can solve the CNLP by only deep

learning infrastructure without using any standard CNLP solvers or numerical integration solvers.

- We propose a dedicated algorithm to train the OINN model toward solving the CNLP. This algorithm is based on the epsilon metric, which is used to evaluate approximate solutions to the CNLP.
- We present the difference between OINN and numerical integration methods for solving a CNLP. OINN can give an approximate solution at any round of iterations, while the numerical integration methods can only give the solution at the end of the program. We show the computational advantages of OINN thanks to this feature.

The remaining sections are organized as follows. The background information necessary to understand this paper is provided in Section 2, including an introduction of CNLPs, neurodynamic optimization methods, and numerical integration methods. Section 3 describes the OINN model and how it solves a CNLP. Training of the OINN model is given in Section 4. Experimental results are given in Section 5 where six different CNLP instances are solved with OINN, and a comparison between OINN and numerical integration methods is presented. Section 6 summarizes this paper and gives future directions.

1.2. Notations

The notations list for this paper is shown in Table 1.

Notation	Definition
$\mathbf{y} \in \mathbb{R}^n$	Variables of a CNLP. n refers to the number of variables.
$\mathbf{y}^* \in \mathbb{R}^n$	Optimal solution of a CNLP.
$\mathbf{x} \in \mathbb{R}^j, \mathbf{u} \in \mathbb{R}^k$	Primal variables and dual variables of a standard CNLP. j refers to the number of primary variables, k refers to the number of dual variables
$P(\cdot)$	A projection function that map variables onto a feasible set.
$\Phi(\mathbf{y}) = \frac{d\mathbf{y}}{dt} : \mathbb{R}^n \rightarrow \mathbb{R}^n$	An ODE system
$\bar{\mathbf{y}}(t) : \mathbb{R} \rightarrow \mathbb{R}^n$	True state solution of an ODE system
$\hat{\mathbf{y}}(t) : \mathbb{R} \rightarrow \mathbb{R}^n$	Approximate state solution obtained by numerical integration methods
$\mathbf{y}(t; \mathbf{w})$	An OINN model, where \mathbf{w} are the model parameters
$\mathbf{y}(T; \mathbf{w}) \in \mathbb{R}^n$	The endpoint of an OINN model
$\mathbf{y}_0 \in \mathbb{R}^n$	An initial point of an ODE system
$[0, T] \subset \mathbb{R}$	A time range of an ODE system
$\epsilon(\cdot)$	Epsilon metric for evaluating a solution of CNLP
$\mathcal{L}(t; \mathbf{w})$	Loss function of OINN
$E(\mathbf{w})$	Objective function of OINN
OINN	Optimization-informed neural networks
CNLP	Constrained nonlinear optimization problem
ODE	Ordinary differential equation
IVP	Initial value problem
NPE	Nonlinear projection equation

Table 1: Notations

2. Preliminaries

Sveral types of CNLP are introduced in Section 2.1. Neurodynamic optimization methods, which model a CNLP as an ODE system, are introduced in Section 2.2. The initial value problem and numerical integration methods are described in Section 2.3.

2.1. Constrained nonlinear optimization problems

This subsection introduces four types of CNLP, i.e., standard CNLP, variational inequality, nonlinear complementary problem, and nonlinear projection equation.

Standard CNLP The standard CNLP has the following form

$$\begin{cases} \min_{\mathbf{x}} f(\mathbf{x}) \\ \text{s.t.} \\ g(\mathbf{x}) \leq \mathbf{0}, \\ \mathbf{Ax} = \mathbf{b}, \end{cases} \quad (1)$$

where $\mathbf{x} \in \mathbb{R}^j$ is the primal variable, $\mathbf{u} \in \mathbb{R}^k$ is the dual variable associated with the constraint $g(\mathbf{x})$. The objective function $f(\mathbf{x}) : \mathbb{R}^j \rightarrow \mathbb{R}$ is not necessary convex or smooth. The constraint function $g(\mathbf{x}) : \mathbb{R}^j \rightarrow \mathbb{R}^k$ is convex but not necessarily smooth, $\mathbf{A} \in \mathbb{R}^{e \times j}$ and $\mathbf{b} \in \mathbb{R}^e$. The following projection function can project the variable \mathbf{x} onto the equality constraints feasible set $\{\mathbf{x} \in \mathbb{R}^j \mid \mathbf{Ax} = \mathbf{b}\}$

$$P_{eq}(\mathbf{x}) = \mathbf{x} - \mathbf{A}^T (\mathbf{AA}^T)^{-1} (\mathbf{Ax} - \mathbf{b}). \quad (2)$$

The standard CNLP (1) is the most common form of CNLP, and we can classify it according to the property of the objective and constraint functions. For example, it is called quadratic programming if the objective function is quadratic and the constraints are linear; Nonsmooth optimization problems are those that involve non-smooth functions.

Nonlinear projection equation (NPE) A NPE aims at finding a vector $\mathbf{y}^* \in \mathbb{R}^n$ such that satisfies

$$P_{\Omega}(\mathbf{y} - G(\mathbf{y})) = \mathbf{y}, \quad (3)$$

where $\mathbf{y} \in \mathbb{R}^n$ is a real vector, $G(\cdot) : \mathbb{R}^n \rightarrow \mathbb{R}^n$ is a locally Lipschitz continuous function, $\Omega = \{\mathbf{y} \in \mathbb{R}^n \mid l_i^- \leq y_i \leq l_i^+, i = 1, \dots, n\}$ is a box-constrained feasible set, where l_i^- and l_i^+ are the lower and upper bounds of y_i , respectively. $P_{\Omega}(\cdot) : \mathbb{R}^n \rightarrow \Omega$ is a projection function that project the variable onto the feasible set Ω ,

defined by

$$P_{\Omega}(\mathbf{s}) = (P_{\Omega}^1(s_1), \dots, P_{\Omega}^n(s_n))^T, \quad \text{where } P_{\Omega}^i(s_i) = \begin{cases} l_i^-, & \text{if } s_i < l_i^- \\ s_i, & \text{if } l_i^- \leq s_i \leq l_i^+ \\ l_i^+, & \text{otherwise.} \end{cases} \quad (4)$$

Variational inequality (VI) A VI aims at finding a vector $\mathbf{y}^* \in \Omega$ such that the following inequalities hold

$$(\mathbf{y} - \mathbf{y}^*)^T G(\mathbf{y}^*) \geq 0, \quad \mathbf{y} \in \Omega. \quad (5)$$

where $G(\cdot)$ and Ω are the same as in (3). Variational inequality provides a reformulation of the Nash equilibrium in game theory to study equilibrium properties, including existence, uniqueness, and convergence (Patriksson, 2013; Parise & Ozdaglar, 2019; Singh & Lisser, 2018).

Nonlinear complementary problem (NCP) A NCP is to find out a vector \mathbf{y}^* that satisfies

$$G(\mathbf{y}) \geq 0, \quad \mathbf{y} \geq 0, \quad G(\mathbf{y})^T \mathbf{y} = 0. \quad (6)$$

where $G(\cdot)$ is the same as in (3). Nonlinear complementarity problems arise in many practical applications. For example, finding a Nash equilibrium is a special case of the Linear complementarity problem; KKT systems of mathematical programming problems can be formulated as NCP problems.

Both the variational inequality (5) and nonlinear complementary problem (6) can be reformulated as an NPE problem (Harker & Pang, 1990; Robinson, 1992). In addition, when the objective and constraint functions are convex and smooth, the CNLP (1) can also be reformulated as an NPE problem, where the variable vector is composed by the primal and dual variable, i.e., $\mathbf{y} = (\mathbf{x}^T, \mathbf{u}^T)^T$.

2.2. Neurodynamic optimization

This subsection introduces neurodynamic optimization methods, which model a CNLP by an ODE system. Consider a CNLP with an optimal solution \mathbf{y}^* . A neurodynamic approach establishes a dynamical system in the form of a first-order ODE system, i.e., $\frac{d\mathbf{y}}{dt} = \Phi(\mathbf{y})$. The state solution $\mathbf{y}(t)$ is expected to converge to the optimal solution of the CNLP, i.e., $\lim_{t \rightarrow \infty} \mathbf{y}(t) = \mathbf{y}^*$. Here, we present three different neurodynamic approaches (Xia & Feng, 2007; Qin & Xue, 2014; Xu et al., 2020), each of which solves a type of CNLP.

Definition 1. Consider an ODE system $\frac{d\mathbf{y}}{dt} = \Phi(\mathbf{y})$, where $\Phi(\mathbf{y}) : \mathbb{R}^n \rightarrow \mathbb{R}^n$. Given a point $(t_0, \mathbf{y}_0) \in \mathbb{R}^{n+1}$, a vector value function $\mathbf{y}(t) : \mathbb{R} \rightarrow \mathbb{R}^n$ is called a state solution, if it satisfies the ODE system $\frac{d\mathbf{y}}{dt} = \Phi(\mathbf{y})$ and the initial condition $\mathbf{y}(t_0) = \mathbf{y}_0$.

Xia & Feng (2007) proposed a neurodynamic approach to model the nonlinear projection equation (3). The ODE system is as follows

$$\frac{d\mathbf{y}}{dt} = \lambda(-G(P_{\Omega}(\mathbf{y})) + P_{\Omega}(\mathbf{y}) - \mathbf{y}), \quad (7)$$

where $\lambda > 0$ is a parameter controlling the convergence rate.

Qin & Xue (2014) proposed a neurodynamic approach to model the standard CNLP (1) when the objective function $f(\cdot)$ and the constraint function $g(\cdot)$ are convex and nonsmooth. The ODE system is as follows

$$\begin{aligned}\frac{d\mathbf{x}}{dt} &\in -(\mathbf{I} - \mathbf{U}) [\partial f(\mathbf{x}) + \partial g(\mathbf{x})^T(\mathbf{u} + g(\mathbf{x}))^+] - \mathbf{A}^T \rho(\mathbf{A}\mathbf{x} - \mathbf{b}), \\ \frac{d\mathbf{u}}{dt} &= \frac{1}{2} (-\mathbf{u} + (\mathbf{u} + g(\mathbf{x}))^+),\end{aligned}\tag{8}$$

where $\mathbf{U} = \mathbf{A}^T (\mathbf{A}\mathbf{A}^T)^{-1} \mathbf{A}$, \mathbf{I} is the identity matrix, and $\rho(\cdot)$ is defined as

$$\rho(\mathbf{s}) = (\tilde{\rho}(s_1), \tilde{\rho}(s_2), \dots, \tilde{\rho}(s_e))^T, \quad \text{where } \tilde{\rho}(s_i) = \begin{cases} 1, & \text{if } s_i > 0 \\ [-1, 1], & \text{if } s_i = 0 \\ -1, & \text{otherwise} \end{cases}\tag{9}$$

Xu et al. (2020) proposed a neurodynamic approach to model the standard CNLP (1) when the objective function $f(\cdot)$ is a pseudoconvex nonsmooth function, and the constraint function $g(\cdot)$ is a convex nonsmooth function. Unlike (8), the ODE system only models the state of \mathbf{x} without considering \mathbf{u} . It is defined as follows

$$\frac{d\mathbf{x}}{dt} \in -\theta(t)(\mathbf{I} - \mathbf{U}) \left(\left\{ \prod_{i=1}^k (1 - \mu(g_i(\mathbf{x}))) \right\} \partial f(\mathbf{x}) + \partial B(\mathbf{x}) \right) - \mathbf{A}^T \rho(\mathbf{A}\mathbf{x} - \mathbf{b}),\tag{10}$$

where $U = \mathbf{A}^T (\mathbf{A}\mathbf{A}^T)^{-1} \mathbf{A}$, and $\rho(\cdot)$ is the same as in (9). $\theta(t)$ is defined by

$$\theta(t) = \begin{cases} 0, & \text{if } t \leq T_0 \\ 1, & \text{otherwise} \end{cases}\tag{11}$$

where $T_0 = 1 + \|\mathbf{A}\mathbf{x}_0 - \mathbf{b}\|_1 / \lambda_{\min}(\mathbf{A}\mathbf{A}^T)$, \mathbf{x}_0 is an initial point, $\lambda_{\min}(\mathbf{A}\mathbf{A}^T) = \min\{\lambda : \lambda \text{ is the eigenvalue of } \mathbf{A}\mathbf{A}^T\}$. $\mu(\cdot)$ is defined by

$$\mu(s) = \begin{cases} 1, & \text{if } s > 0 \\ [0, 1], & \text{if } s = 0 \\ 0, & \text{if } s < 0 \end{cases}\tag{12}$$

$\partial B(\mathbf{x})$ is given by

$$\partial B(\mathbf{x}) = \begin{cases} \{0\}, & \mathbf{x} \in S \cap \text{int}(\mathcal{F}) \\ \sum_{i \in I^0(\mathbf{x})} \mu(g_i(\mathbf{x})) \partial g_i(\mathbf{x}), & \mathbf{x} \in S \cap \text{bd}(\mathcal{F}) \\ \sum_{i \in I^0(\mathbf{x})} \mu(g_i(\mathbf{x})) \partial g_i(\mathbf{x}) + \sum_{i \in I^+(\mathbf{x})} \partial g_i(\mathbf{x}), & \mathbf{x} \in S \setminus \mathcal{F} \end{cases}\tag{13}$$

where $\mathcal{F} = \{\mathbf{x} : g_i(\mathbf{x}) \leq 0, i = 1, 2, \dots, k\}$, $S = \{x : \mathbf{A}x = \mathbf{b}\}$, $I^0(\mathbf{x}) = \{i \in \{1, 2, \dots, k\} : g_i(\mathbf{x}) = 0\}$, $I^+(\mathbf{x}) = \{i \in \{1, 2, \dots, k\} : g_i(\mathbf{x}) > 0\}$.

Reference	Neurodynamic approach			CNLP	Conditions on functions
	ODE system	Projection	Global convergence		
Xia & Feng (2007)	(7)	(4)	True	(1), (3) (5), (6)	In (1), $f(\cdot)$ and $g(\cdot)$ are convex and smooth In (3), (5), (6), $G(\cdot)$ is locally lipschitz.
Qin & Xue (2014)	(8)	(2)	True	(1)	In (1), $f(\cdot)$ and $g(\cdot)$ are convex and nonsmooth
Xu et al. (2020)	(10)	(2)	True	(1)	In (1), $f(\cdot)$ and $g(\cdot)$ are pseudoconvex and smooth

Table 2: **Summary of the neurodynamic approaches and their corresponding CNLPs.** Global convergence refers to whether the ODE system can globally converge to the solution set of the CNLP. Conditions on functions refer to the assumptions required for the CNLP.

Definition 2. An ODE system $\frac{dy}{dt} = \Phi(\mathbf{y})$ is said to be globally converges to a solution set \mathcal{Y}^* if for any given initial point, the state solution $\mathbf{y}(t)$ satisfies

$$\lim_{t \rightarrow \infty} \text{dist}(\mathbf{y}(t), \mathcal{Y}^*) = 0,$$

where $\text{dist}(\mathbf{y}(t), \mathcal{Y}^*) = \inf_{\mathbf{y}^* \in \mathcal{Y}^*} \|\mathbf{y}(t) - \mathbf{y}^*\|$, and $\|\cdot\|$ is the euclidean norm. In particular, if the set \mathcal{Y}^* contains only one point \mathbf{y}^* , then $\lim_{t \rightarrow \infty} \mathbf{y}(t) = \mathbf{y}^*$, and the ODE system is globally asymptotically stable at \mathbf{y}^* .

The global convergence property states that starting from any initial point, the state solution $\mathbf{y}(t)$ of the ODE system converges to the CNLP solution as time t goes to infinity. A neurodynamic approach usually establishes the global convergence property in two steps: First, the ODE system’s equilibrium points coincide with the optimal solutions of the CNLP. Then, using Lyapunov’s theorem or LaSalle’s invariance principle to prove that any state solution will converge to an equilibrium point of the ODE system.

Table 2 summarizes these three neurodynamic optimization methods and their target CNLPs. Projection (4) is presented in the original paper of Xia & Feng (2007), and we add the Projection (2) to facilitate the use of deep learning later. All three neurodynamic methods have the global convergence property. We refer the reader to (Xia & Feng, 2007; Qin & Xue, 2014; Xu et al., 2020) for the proof of the global convergence theorems and other details.

2.3. Initial value problem

An initial value problem (IVP) is an ODE system together with an initial point and a time range. The solution to the IVP is called a state solution that satisfies the initial point and the ODE system over the time range.

Almost all the ODE systems considered in this paper are nonlinear and cannot be solved analytically. Therefore, in practice, the IVP is usually solved by numerical integration methods, which approximate the state solution by the discretization of the domain. (Butcher, 2016). As a typical example, Runge-Kutta methods numerically integrate the ODE system by starting with the initial point and moving forward until the desired final time is reached. The numerical integration method chooses a number of time points in the

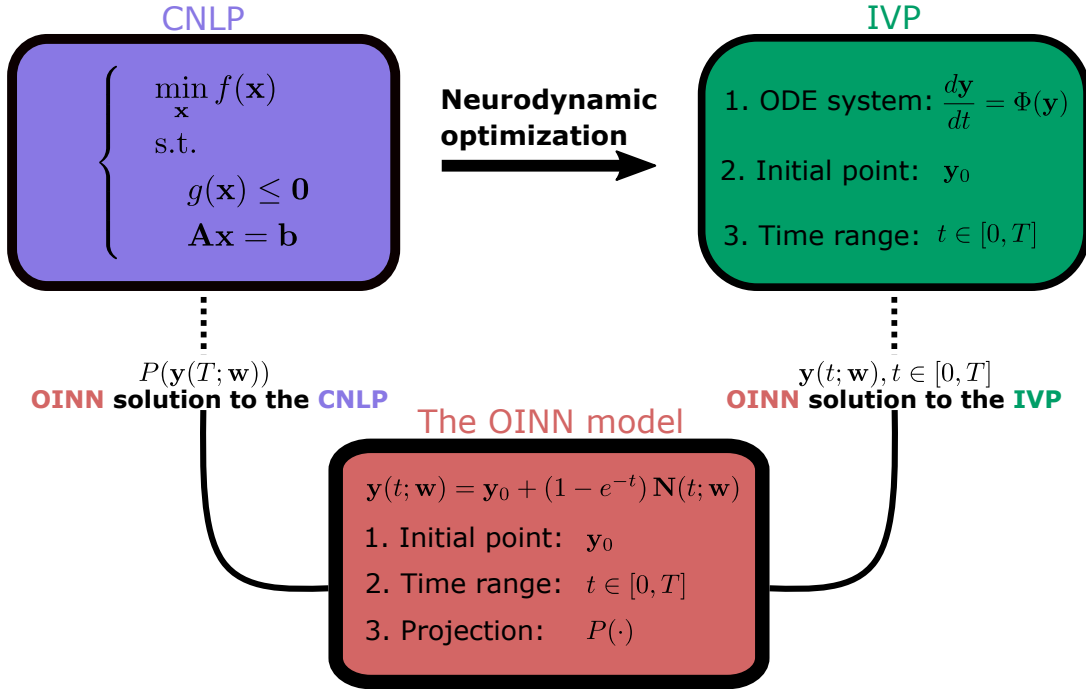


Figure 1: **Problem set-up and OINN solution** The demonstrated CNLP is a standard CNLP, where \mathbf{x} is primal variables, and \mathbf{u} is dual variables. \mathbf{y} is composed of \mathbf{x} and \mathbf{u} , i.e., $\mathbf{y} = [\mathbf{x}, \mathbf{u}]$.

domain, called collocation points, and then find a solution that satisfies the ODE system at these points. However, these conventional methods are inefficient if only the state at the end is of interest. This is due to the significant computational work required to determine all the ahead collocation points.

Numerical integration methods are divided into two categories: explicit and implicit methods. The explicit methods determine the system's state at a later time based on the current state, e.g., RK45, RK23, and DOP853 (Dormand & Prince, 1980; Bogacki & Shampine, 1989; Hairer et al., 1993). The implicit methods find the solution by solving equations involving the current and later states, e.g., Radau and BDF (Wanner & Hairer, 1996; Shampine & Reichelt, 1997). In addition, LSODA can switch automatically between stiff and nonstiff methods (Petzold, 1983). Scipy provides software implementations of these methods to facilitate their use (Virtanen et al., 2020).

3. OINN model

OINN is a generic framework for solving different CNLPs by working with neurodynamic optimization methods. As shown in Figure1, a standard CNLP is first reformulated as an IVP. Then, an OINN model is built to solve both the CNLP and IVP. Let \mathbf{y}^* be the optimal solution of the CNLP, $\bar{\mathbf{y}}(t)$ be the state solution of the IVP. In this section, we show how an OINN model provides approximations for \mathbf{y}^* and $\bar{\mathbf{y}}(t)$.

OINN solution to the IVP The OINN model is defined as follows

$$\mathbf{y}(t; \mathbf{w}) = \mathbf{y}_0 + (1 - e^{-t})\mathbf{N}(t; \mathbf{w}), \quad (14)$$

where $\mathbf{y}_0 \in \mathbb{R}^n$ is an initial point, $[0, T] \subseteq \mathbb{R}$ is a time range, and $t \in [0, T]$ is the time variable. $(1 - e^{-t})$ ensures that the OINN model always satisfies the initial condition, i.e., $\mathbf{y}(0; \mathbf{w}) = \mathbf{y}_0$. This construction method is initially introduced by Lagaris et al. (1998), and Mattheakis et al. (2022) demonstrates that the exponential form can result in better convergence. $\mathbf{N}(t; \mathbf{w})$ is a neural network with learnable parameters \mathbf{w} . This paper considers the fully connected network only; other network structures are worth investigating in future research. The OINN model itself is an approximate state solution to the IVP, i.e.,

$$\mathbf{y}(t; \mathbf{w}) \approx \bar{\mathbf{y}}(t), \quad t \in [0, T] \quad (15)$$

OINN solution to the CNLP By the neurodynamic optimization method, the endpoint of the state solution is an approximation of the optimal solution of the CNLP, i.e.,

$$\bar{\mathbf{y}}(T) \approx \mathbf{y}^* \quad (16)$$

Combining the endpoint $t = T$ of (15) and (16), we have

$$P(\mathbf{y}(T; \mathbf{w})) \approx \mathbf{y}^*, \quad (17)$$

where $P(\cdot)$ is a projection function that projects the endpoint onto a feasible set, e.g., the box-constraints (4) and the equality-constraints (2). The expression (17) represents that the endpoint of the OINN model, together with a projection function, is an approximate solution to the optimal solution of the CNLP.

Here, we discuss two newly introduced hyperparameters in OINN, namely the initial point and the time range.

Initial point \mathbf{y}_0 Any initial point can converge to the optimal solution as long as the time goes to infinity, according to the global convergence property. Therefore, the choice of the initial point does not affect the convergence. However, the initial point selection has a significant impact on convergence speed; the closer the initial point is to the optimal solution, the faster the state solution approaches it.

Time range $[0, T]$ The time range determines the training difficulty and the upper limit of accuracy. For training difficulty, since the time range is exactly the input space of the OINN model, its span determines how large an input space the OINN model needs to be trained on. At the same time, the time range determines the location of the state solution endpoint $\bar{\mathbf{y}}(T)$, which in turn represents an upper limit of accuracy. Therefore, the choice of the time range span is a trade-off. On the one hand, the long span enables the OINN model to provide a better solution, but more training iterations are necessary to achieve it. On the other hand, the short span is simpler to train, but the OINN model might not achieve the desired accuracy, no matter how many training iterations.

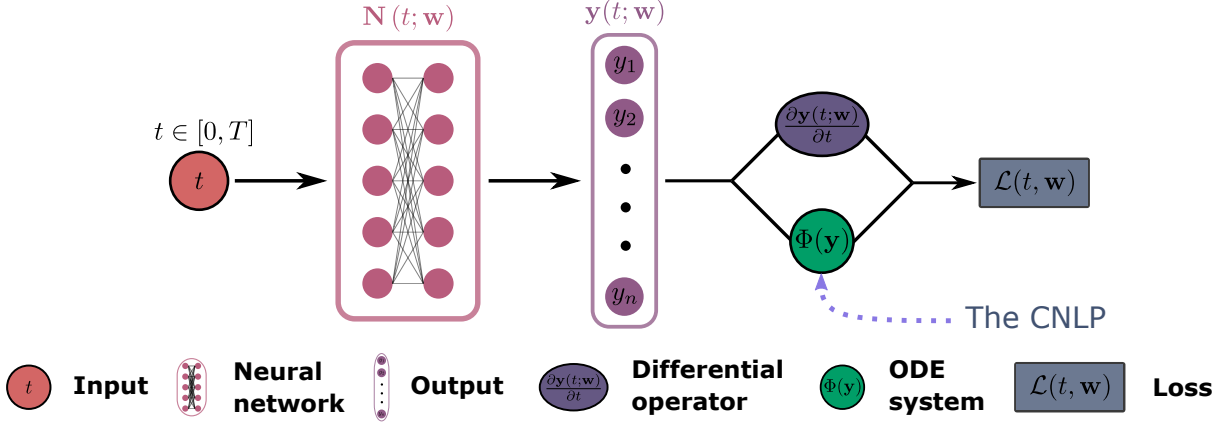


Figure 2: Computational flow of the loss function

4. OINN training

4.1. Loss function

The loss function of the OINN model is defined as follows

$$\mathcal{L}(t, \mathbf{w}) = e^{-\gamma * t} \left\| \frac{\partial \mathbf{y}(t; \mathbf{w})}{\partial t} - \Phi(\mathbf{y}(t; \mathbf{w})) \right\|, \quad (18)$$

where $\Phi(\cdot)$ refers to the ODE system corresponding to the CNLP. $\frac{\partial \mathbf{y}(t; \mathbf{w})}{\partial t}$ is the derivative of the output $\mathbf{y}(t; \mathbf{w})$ with respect to the input time t , which can be computed analytically. The multiplier $e^{-\gamma * t}$ reassigns the weights in the loss and gives a higher weight to the time closer to the origin, where γ is a weighting hyperparameter. Using such a multiplier comes from the fact that global error can grow exponentially as a result of an early local error (Flamant et al., 2020). Figure 2 illustrates the computational flow from a time t to the loss value $\mathcal{L}(t, \mathbf{w})$.

The objective function for the OINN model is given by

$$E(\mathbf{w}) = \int_0^T \mathcal{L}(t, \mathbf{w}) dt. \quad (19)$$

The objective function $E(\mathbf{w})$ is an integral of the loss function over the time range $[0, T]$. The loss value $\mathcal{L}(t, \mathbf{w})$ denotes the error of the OINN model at the time t . The $E(\mathbf{w})$ denotes the overall error of the OINN model over the time range $[0, T]$.

However, training the model by applying gradient descent on $E(\mathbf{w})$ is infeasible since the integral over $[0, T]$ is computationally intractable. One can instead train by minimizing the batch loss

$$\mathcal{L}(\mathbb{T}, \mathbf{w}) = \frac{1}{|\mathbb{T}|} \sum_{t \in \mathbb{T}} \mathcal{L}(t, \mathbf{w}), \quad (20)$$

where \mathbb{T} is a set of time t randomly drawn from $[0, T]$. $|\mathbb{T}|$ denotes to the size of the set.

4.2. Epsilon metric

We propose a method to evaluate how well the OINN solution solves the CNLP, called the epsilon metric. The epsilon metric can be defined in two different ways, depending on the particular CNLP.

Epsilon: Nonlinear projection equation error For a CNLP that can be reformulated as an NPE (3), such as variational inequality and nonlinear complementarity problem, the epsilon value is defined as follows

$$\epsilon_1(\mathbf{y}) = |P_\Omega(\mathbf{y} - \alpha G(\mathbf{y})) - \mathbf{y}|. \quad (21)$$

The epsilon value $\epsilon_1(\mathbf{y})$ indicates how well a solution \mathbf{y} satisfies the equation (3).

Epsilon: Objective value For the standard CNLP (1), the epsilon value can be defined as follows

$$\epsilon_2(\mathbf{y}) = \begin{cases} f(\mathbf{x}) & \text{if } \mathbf{x} \in \mathcal{X}, \\ +\infty & \text{otherwise,} \end{cases} \quad (22)$$

where $\mathbf{y} = [\mathbf{x}, \mathbf{u}]$, \mathcal{X} denotes the feasible set of the standard CNLP. When \mathbf{x} is within the feasible set, the epsilon value $\epsilon_2(\mathbf{y})$ is the objective value; otherwise, it is set to $+\infty$. By utilizing a projection function that maps \mathbf{x} onto some basic feasible set, such as $P_{eq}(\mathbf{x})$ for projecting to the equality constraint set, $\epsilon_2(\mathbf{y})$ can more likely be finite.

4.3. Training algorithm

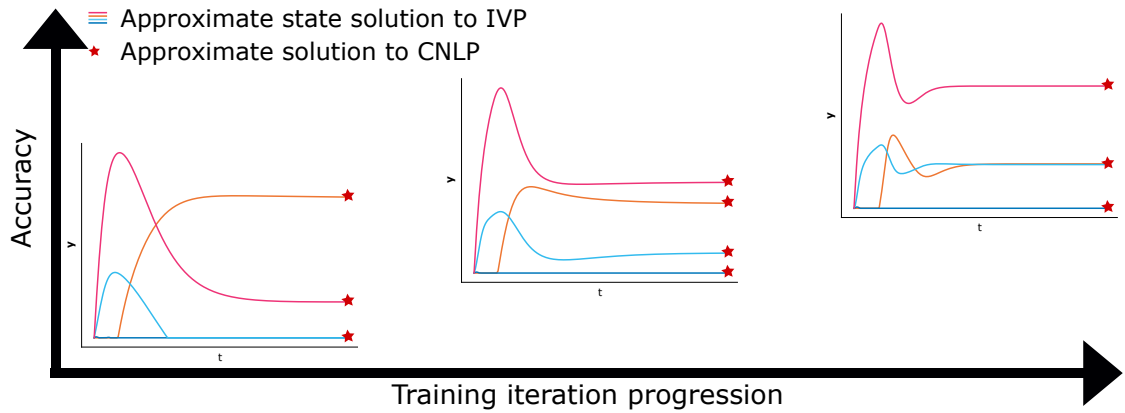
Algorithm 1: Training of an OINN model for solving a CNLP

Hyperparameters: An initial point \mathbf{y}_0 , A time range $[0, T]$
Input : A CNLP
Output : The OINN model after training

- 1 **Function Main:**
- 2 Derive the ODE system $\Phi(\cdot)$ corresponding to the CNLP by a neurodynamic optimization method.
- 3 Initialize an OINN model $\mathbf{y}(t; \mathbf{w})$.
- 4 Initialize $\epsilon_{\text{best}} = P(\mathbf{y}(T; \mathbf{w}))$.
- 5 **while** $\text{iter} \leq \text{Max iteration}$ **do**
- 6 $\mathbb{T} \sim U(0, T)$: Uniformly sample a batch of t from the interval $[0, T]$.
- 7 Forward propagation: Compute the batch loss $\mathcal{L}(\mathbb{T}, \mathbf{w})$.
- 8 Backward propagation: Update \mathbf{w} by $\nabla_{\mathbf{w}} \mathcal{L}(\mathbb{T}, \mathbf{w})$.
- 9 Compute the epsilon value: $\epsilon_{\text{temp}} = P(\mathbf{y}(T; \mathbf{w}))$.
- 10 **if** $\epsilon_{\text{temp}} < \epsilon_{\text{best}}$ **then**
- 11 $\epsilon_{\text{best}} = \epsilon_{\text{temp}}$
- 12 Save the OINN model with parameters \mathbf{w}
- 13 **end**
- 14 **end**

Algorithm 1 presents an optimization procedure for the objective function $E(\mathbf{w})$ combined with the epsilon metric. At each iteration, a batch of t is sampled uniformly from the time range $[0, T]$ as an input dataset.

(A) OINN training



(B) Numerical intergration method

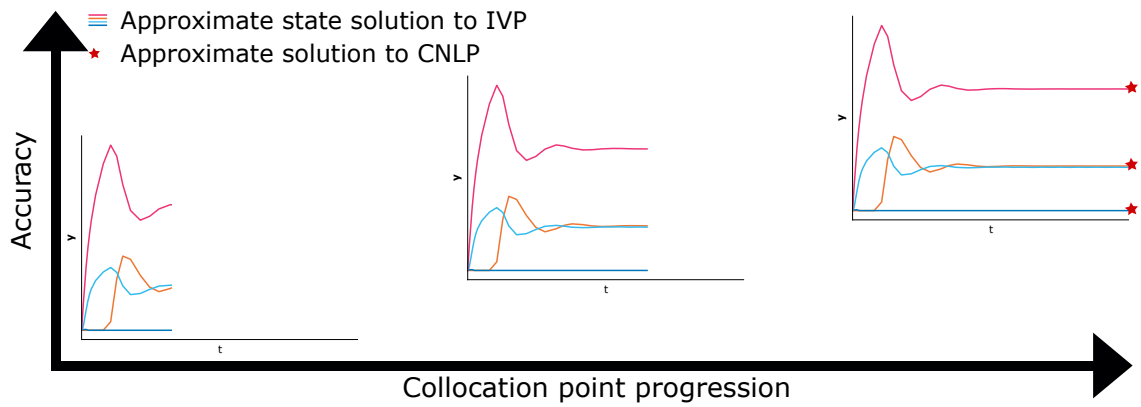


Figure 3: Comparison between OINN and the numerical integration method for solving a CNLP

Then, the OINN model performs gradient descent on the batch loss $\mathcal{L}(\mathbb{T}, \mathbf{w})$, which is an unbiased estimate of $E(\mathbf{w})$.

After each round of training, the epsilon value of the OINN solution to the CNLP is computed, i.e., $\epsilon_{\text{temp}} = \epsilon(P(\mathbf{y}(T; \mathbf{w})))$, where $\epsilon(\cdot)$ is defined by either (21) or (22). Throughout the training process, the algorithm maintains the lowest epsilon value, namely ϵ_{best} , representing the best solution, and the corresponding model parameter is saved. This idea is similar to the *early-stopping* in deep learning, except here, we consider the epsilon value rather than the loss.

As the OINN training progresses, the model increases its accuracy for the IVP; the prediction accuracy to the CNLP is improved by solving the IVP, as shown in Figure 3-(A). The numerical integration method solves the IVP by stepwise integrating the ODE system and returns the solution to the CNLP at the end of the program, as shown in Figure 3-(B). One of the promising features of OINN is that it can provide approximations for the IVP and the CNLP at any training iteration, while the numerical method can only produce solutions at the end of the program.

5. Numerical experiments

We use the Google Colab Pro+ platform to conduct our experiments, Pytorch 1.9.1 as the deep learning library. Jax 0.3.0 is used as an automatic differentiation tool to compute the gradient or the Jacobian of a given function and subsequently models the ODE system (Bradbury et al., 2018).

The training hyperparameters are as follows

- The optimizer is ADAM with a learning rate of 0.001. The decay weighting is $\gamma = 0.5$.
- The batch size is 512, and the maximum number of iterations is 50000.
- The structure of each OINN model is a fully-connected neural network with one hidden layer of 100 neurons and Tanh as the activation function.

In the following, Section 5.1 shows how to use OINN to solve six different CNLP examples. Section 5.2 performs a hyperparameter study on the initial point \mathbf{y}_0 and time range $[0, T]$. Section 5.3 compares the OINN method with the numerical integration methods.

5.1. Six CNLP examples

5.1.1. Quadratic programming

Example 1. Consider the following quadratic programming problem

$$\begin{aligned} \min_{\mathbf{x}} f(\mathbf{x}) &= \frac{1}{2}\mathbf{x}^T Q \mathbf{x} + p^T \mathbf{x} \\ \text{s.t.} & \\ C\mathbf{x} &\leq d \\ \mathbf{x} &\geq 0, \end{aligned} \tag{23}$$

where

$$Q = \begin{bmatrix} 18 & 9 & 13 \\ 9 & 14 & 6 \\ 13 & 6 & 10 \end{bmatrix}, \quad p = \begin{bmatrix} -30 \\ -30 \\ 15 \end{bmatrix}, \quad C = \begin{bmatrix} 4 & -5 & -4 \\ -5 & -2 & -4 \end{bmatrix}, \quad d = \begin{bmatrix} -5 \\ 1 \end{bmatrix}.$$

The CNLP (23) can be reformulated as the NPE as follows

$$(\mathbf{y} - (M\mathbf{y} + q))^+ = \mathbf{y}, \tag{24}$$

where $\mathbf{y} = [x_1, x_2, x_3, u_1, u_2]^T$, x_1 , x_2 and x_3 are decision variables, and u_1 , u_2 are dual variables. $(\mathbf{y})^+ = \max\{\mathbf{0}, \mathbf{y}\}$. M and q are denoted as

$$M = \begin{bmatrix} Q & C^T \\ -C & 0 \end{bmatrix}, \quad q = \begin{bmatrix} p \\ d \end{bmatrix}.$$

The following ODE system model the NPE

$$\frac{dy}{dt} = -M(y)^+ - q + (y)^+ - y. \quad (25)$$

The ODE system together with the initial point $\mathbf{y}_0 = [0, 0, 0, 0, 0]$ and time range $[0, 10]$ form the IVP as follow

$$(25), \quad \mathbf{y}_0 = [0, 0, 0, 0, 0], \quad t \in [0, 10] \quad (26)$$

An OINN model, $\mathbf{y}(t; \mathbf{w}) \quad t \in [0, 10]$, is built as an approximate state solution to the IVP (26), and its endpoint $(\mathbf{y}(10; \mathbf{w}))^+$ is an approximate solution to the NPE (24).

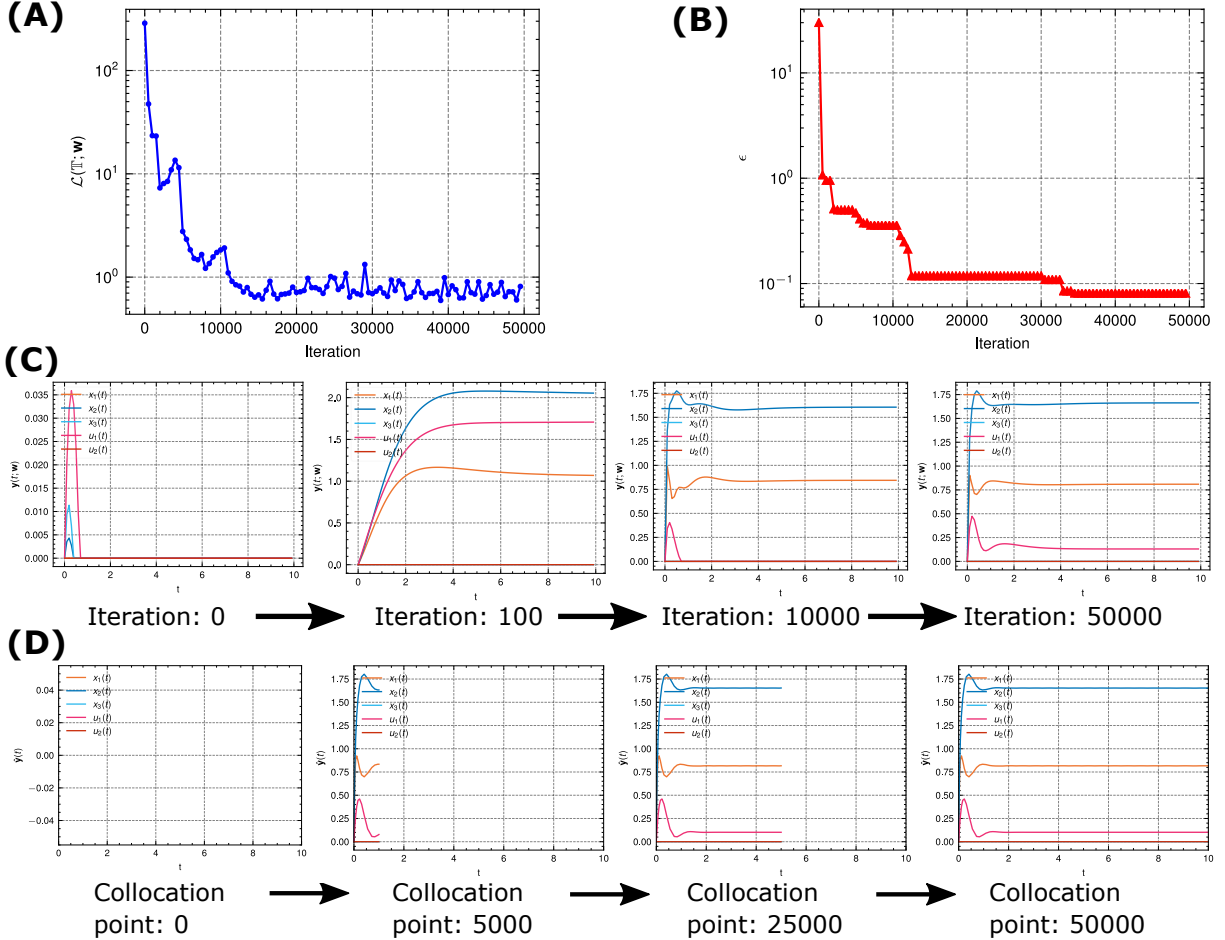


Figure 4: **Example 1 Quadratic programming** (A) The loss versus the number of iterations. $\mathcal{L}(\mathbb{T}, \mathbf{w})$ refers to the batch loss defined in (20) and (18) (B) The epsilon value versus the number of iterations. The epsilon metric is defined in (21) (C) The solving process of the OINN model (D) The solving process of the numerical integration method

Figure 4 shows the training of this OINN model, where the loss decreased from the initial value of 287.26 to 0.62, and the epsilon value decreased from 30.00 to 0.08. Figure 4 (C) and (D) show the progressions of

Index	OINN		Numerical integration method	
	Iteration	Solution	Collocation point	Solution
Example 1	0	[0.00, 0.00, 0.00, 0.00, 0.00]	0	[0.00, 0.00, 0.00, 0.00, 0.00]
	10	[0.00, 0.42, 0.00, 0.17, 0.00]	10	[0.06, 0.06, 0.00, 0.01, 0.00]
	100	[1.07, 2.05, 0.00, 1.71, 0.00]	100	[0.46, 0.49, 0.00, 0.09, 0.00]
	1000	[0.75, 1.73, 0.00, 0.00, 0.00]	1000	[0.82, 1.63, 0.00, 0.46, 0.00]
	10000	[0.84, 1.61, 0.00, 0.00, 0.00]	10000	[0.82, 1.65, 0.00, 0.10, 0.00]
	50000	[0.81, 1.66, 0.00, 0.13, 0.00]	50000	[0.82, 1.65, 0.00, 0.10, 0.00]

Table 3: **Example 1, Approximate solutions to the NPE during solving** We choose a step size of 0.0002 for the numerical integration method. collocation points 0, 10, 100, 1000, 10000, 50000 represent the time ranges [0, 0], [0, 0.002], [0, 0.2], [0, 2], [0, 10] respectively.

the approximate state solutions to the IVP (26).

Table 3 displays the progressions of the approximate solutions to the NPE (24). The OINN model gives the final solution of [0.81, 1.66, 0.00, 0.13, 0.00] to the NPE, where [0.81, 1.66, 0.00] is the solution to the CNLP (23). The numerical integration method gives the final solution of [0.82, 1.65, 0.00, 0.10, 0.00] to the NPE, where [0.82, 1.65, 0.00] is the solution to the CNLP (23).

5.1.2. Convex-smooth standard CNLP

Example 2. Consider the following convex-smooth standard CNLP:

$$\begin{aligned}
\min_{\mathbf{x}} f(\mathbf{x}) &= x_1^2 + 2x_2^2 + 2x_1x_2 - 10x_1 - 12x_2 \\
\text{s.t.} \\
g_1(\mathbf{x}) &= x_1 + 3x_2 - 8 \leq 0 \\
g_2(\mathbf{x}) &= x_1^2 + x_2^2 + 2x_1 - 2x_2 - 3 \leq 0 \\
0 &\leq \mathbf{x} \leq 2.
\end{aligned} \tag{27}$$

The CNLP can be reformulated as the following NPE

$$P_{\Omega}(\mathbf{y} - G(\mathbf{y})) = \mathbf{y}, \tag{28}$$

where $\mathbf{y} = [x_1, x_2, u_1, u_2]^T$; x_1, x_2 are decision variables, and u_1, u_2 are dual variables. $P_{\Omega}(\mathbf{y})$ is a projection function defined in (4) which projects $\mathbf{y} \in \mathbb{R}^4$ onto the set $\Omega = \{\mathbf{y} \in \mathbb{R}^4 \mid 0 \leq x_1 \leq 2, 0 \leq x_2 \leq 2, u_1 \geq 0, u_2 \geq 0\}$. $G(\mathbf{y})$ is defined as

$$G(\mathbf{y}) = \begin{bmatrix} \nabla f(\mathbf{x}) + \nabla g(\mathbf{x})^T \mathbf{u} \\ -g(\mathbf{x}) \end{bmatrix}, \tag{29}$$

where $g(\mathbf{x}) = [g_1(\mathbf{x}), g_2(\mathbf{x})]^T$, $\mathbf{x} = [x_1, x_2]^T$, $\mathbf{u} = [u_1, u_2]^T$.

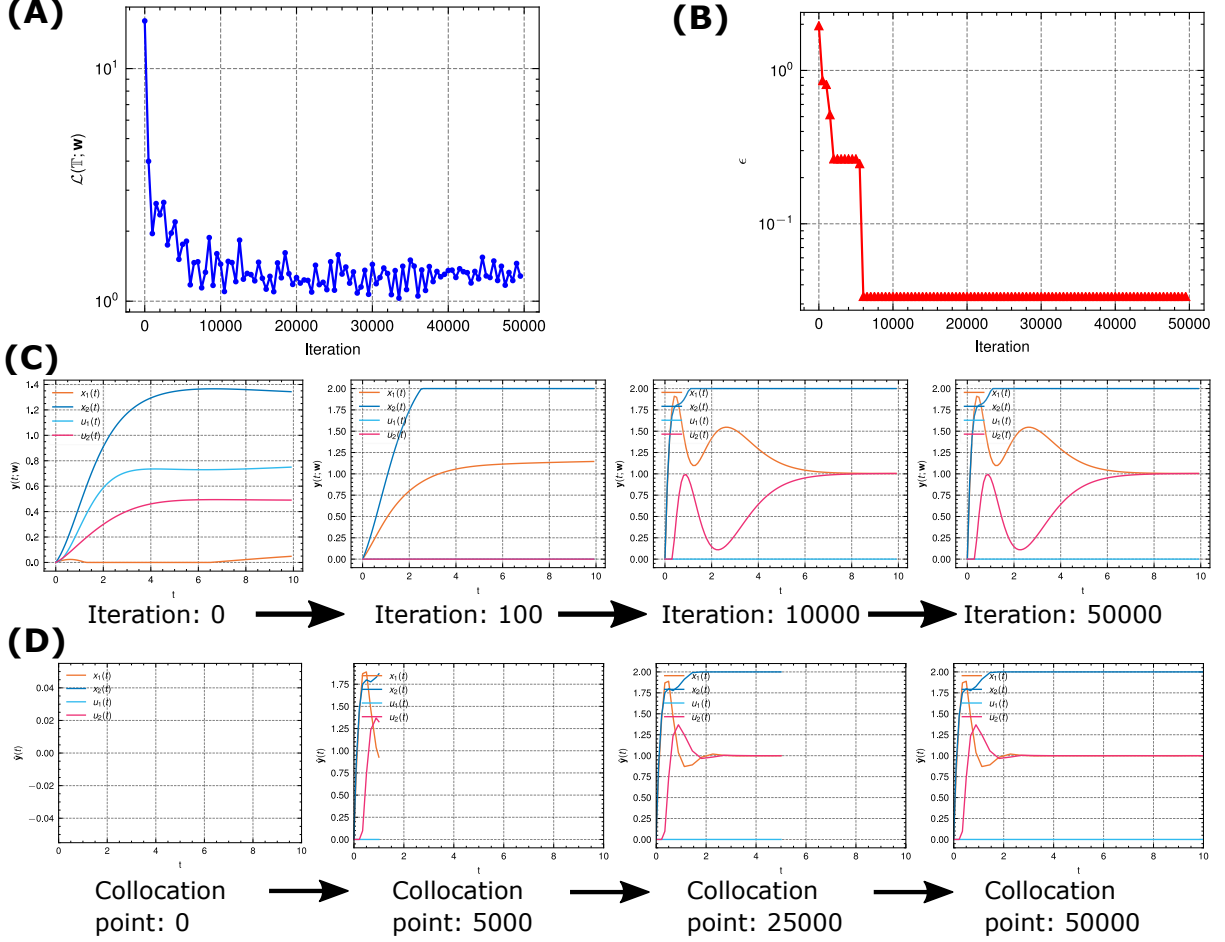


Figure 5: **Example 2 Convex smooth standard CNLP** (A) The loss versus the number of iterations. (B) The epsilon value versus the number of iterations. The epsilon metric is defined in (21) (C) The solving process of the OINN model (D) The solving process of the numerical integration method

The following ODE system models the NPE (28)

$$\frac{dy}{dt} = -G(P_{\Omega}(\mathbf{y})) + P_{\Omega}(\mathbf{y}) - \mathbf{y}, \quad (30)$$

The ODE system together with the initial point $\mathbf{y}_0 = [0, 0, 0, 0]$ and time range $[0, 10]$ form an IVP as follow

$$(30), \quad \mathbf{y}_0 = [0, 0, 0, 0], \quad t \in [0, 10] \quad (31)$$

An OINN model, $\mathbf{y}(t; \mathbf{w})$ $t \in [0, 10]$, is built as an approximate state solution to this IVP (31), and its endpoint $P_{\Omega}(\mathbf{y}(10; \mathbf{w}))$ is an approximate solution to the NPE (28).

Figure 5 shows the training of the OINN model, where the loss value decreased from 16.02 to 1.11, and the epsilon value decreased from 1.95 to 0.03. Figure 5 (C) and (D) show the progressions of the approximate state solutions to the IVP (31).

Index	OINN		Numerical integration method	
	Iteration	Solution	Collocation point	Solution
Example 2	0	[0.05, 1.34, 0.75, 0.49]	0	[0.00, 0.00, 0.00, 0.00]
	10	[0.84, 2.00, 0.00, 0.00]	10	[0.02, 0.02, 0.00, 0.00]
	100	[1.15, 2.00, 0.00, 0.00]	100	[0.19, 0.23, 0.00, 0.00]
	1000	[1.19, 2.00, 0.00, 0.00]	1000	[1.36, 1.42, 0.00, 0.00]
	10000	[1.00, 2.00, 0.00, 1.00]	10000	[1.01, 2.00, 0.00, 0.97]
	50000	[1.00, 2.00, 0.00, 1.00]	50000	[1.00, 2.00, 0.00, 1.00]

Table 4: **Example 2, Approximate solutions to the NPE during solving**

Table 4 displays the progression of the approximate solutions to the NPE (28). Both the OINN model and the numerical integration method gives the same final solution of [1.00, 2.00, 0.00, 1.00] to the NPE (28), where [1.00, 2.00] is the solution to the CNLP (27).

5.1.3. Variational inequality

Example 3. Consider the following variational inequality

$$(\mathbf{y} - \mathbf{y}^*)^T G(\mathbf{y}^*) \geq 0, \quad \mathbf{y} \in \Omega, \quad (32)$$

where

$$G(\mathbf{y}) = \begin{bmatrix} y_1 - \frac{2}{(y_1+0.8)} + 5y_2 - 13 \\ 1.2y_1 + 7y_2 \\ 3y_3 + 8y_4 \\ y_3 + 2y_4 - \frac{4}{(y_4+2)} - 12 \end{bmatrix}, \quad \Omega = \{\mathbf{y} \in \mathbb{R}^4 \mid 1 \leq y_1 \leq 100, -3 \leq y_2 \leq 100, \\ -3 \leq y_3 \leq 100, 1 \leq y_4 \leq 100\}.$$

The problem can be reformulated as the following NPE

$$P_{\Omega}(\mathbf{y} - G(\mathbf{y})) = \mathbf{y}. \quad (33)$$

The following ODE system model the NPE (33)

$$\frac{d\mathbf{y}}{dt} = -G(P_{\Omega}(\mathbf{y})) + P_{\Omega}(\mathbf{y}) - \mathbf{y}. \quad (34)$$

The ODE system together with the initial point $\mathbf{y}_0 = [0, 0, 0, 0]$ and time range $[0, 10]$ form the IVP as follow

$$(34), \quad \mathbf{y}_0 = [0, 0, 0, 0], \quad t \in [0, 10]. \quad (35)$$

An OINN model, $\mathbf{y}(t; \mathbf{w})$ $t \in [0, 10]$, is built as an approximate state solution to this IVP (35), and its

endpoint $P_\Omega(\mathbf{y}(10; \mathbf{w}))$ is an approximate solution to the NPE (33).

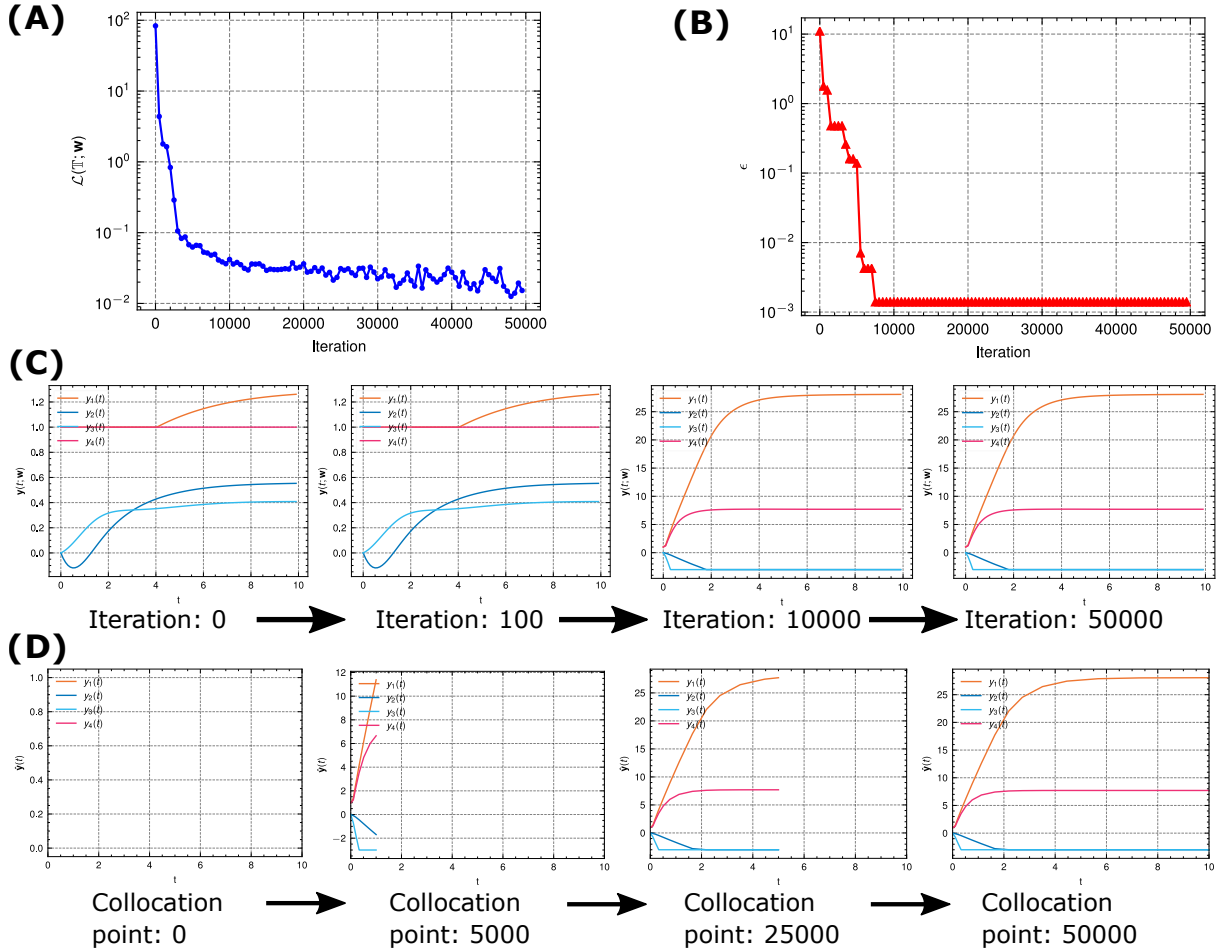


Figure 6: **Example 3** variational inequality (A) The loss versus the number of iterations. (B) The epsilon value versus the number of iterations. The epsilon metric is defined in (21) (C) The solving process of the OINN model (D) The solving process of the numerical integration method

Index	OINN		Numerical integration method	
	Iteration	Solution	Collocation point	Solution
Example 3	0	[1.26, 0.55, 0.41, 1.00]	0	[1.00, 0.00, 0.00, 1.00]
	10	[1.26, 0.55, 0.41, 1.00]	10	[1.00, 0.00, -0.02, 1.00]
	100	[1.26, 0.55, 0.41, 1.00]	100	[1.00, -0.02, -0.16, 1.00]
	1000	[26.52, -3.00, -3.00, 7.67]	1000	[2.61, -0.22, -1.74, 2.28]
	10000	[28.07, -3.00, -3.00, 7.71]	10000	[20.79, -3.00, -3.00, 7.57]
	50000	[28.07, -3.00, -3.00, 7.71]	50000	[28.06, -3.00, -3.00, 7.70]

Table 5: **Example 3**, Approximate solutions to the NPE during solving

Figure 6 shows the training of the OINN model, where the loss value decreased from 83.38 to 0.01, and the epsilon value decreased from 10.92 to 0.00. Figure 6 (C) and (D) show the progression of the approximate state solutions to the IVP (35).

Table 5 displays the progression of the approximate solutions to the NPE (33). The OINN model gives

the final solution of $[28.07, -3.00, -3.00, 7.71]$ to both the variational inequality (32) and NPE (33). The numerical method gives the final solution of $[28.06, -3.00, -3.00, 7.70]$.

5.1.4. Nonlinear complementary problem

Example 4 Consider the following nonlinear complementary problem

$$\mathbf{y}^T F(\mathbf{y}) = 0, \quad F(\mathbf{y}) \geq 0, \quad \mathbf{y} \geq 0, \quad (36)$$

where

$$F(\mathbf{y}) = \begin{pmatrix} 2y_1 e^{(y_1^2 + (y_2 - 1)^2)} + y_1 - y_2 - y_3 + 1 \\ 2(y_2 - 1) e^{(y_1^2 + (y_2 - 1)^2)} - y_1 + 2y_2 + 2y_3 + 3 \\ -y_1 + 2y_2 + 3y_3 \end{pmatrix}.$$

The problem can be reformulated as the following NPE

$$(\mathbf{y} - F(\mathbf{y}))^+ = \mathbf{y}. \quad (37)$$

The following ODE system model the NPE (37)

$$\frac{d\mathbf{y}}{dt} = -F((\mathbf{y})^+) + (\mathbf{y})^+ - \mathbf{y}, \quad (38)$$

The ODE system together with the initial point $\mathbf{y}_0 = [0, 0, 0]$ and time range $[0, 10]$ form the IVP as follow

$$(38), \quad \mathbf{y}_0 = [0, 0, 0], \quad t \in [0, 10] \quad (39)$$

An OINN model, $\mathbf{y}(t; \mathbf{w})$ $t \in [0, 10]$, is built as an approximate state solution to this IVP (39), and its endpoint $P_\Omega(\mathbf{y}(10; \mathbf{w}))$ is an approximate solution to the NPE (37).

Figure 7 shows the training of the OINN model, where the loss value decreased from 0.24 to 0.00, and the epsilon value decreased from 3.12 to 0.00. Figure 7 (C) and (D) display the progression of the approximate state solutions to the IVP (39).

Table 6 displays the progression of the approximate solutions to the NPE (37). The OINN model gives the final solution of $[0.00, 0.17, 0.00]$ for both the nonlinear complementary problem (36) and NPE (37).

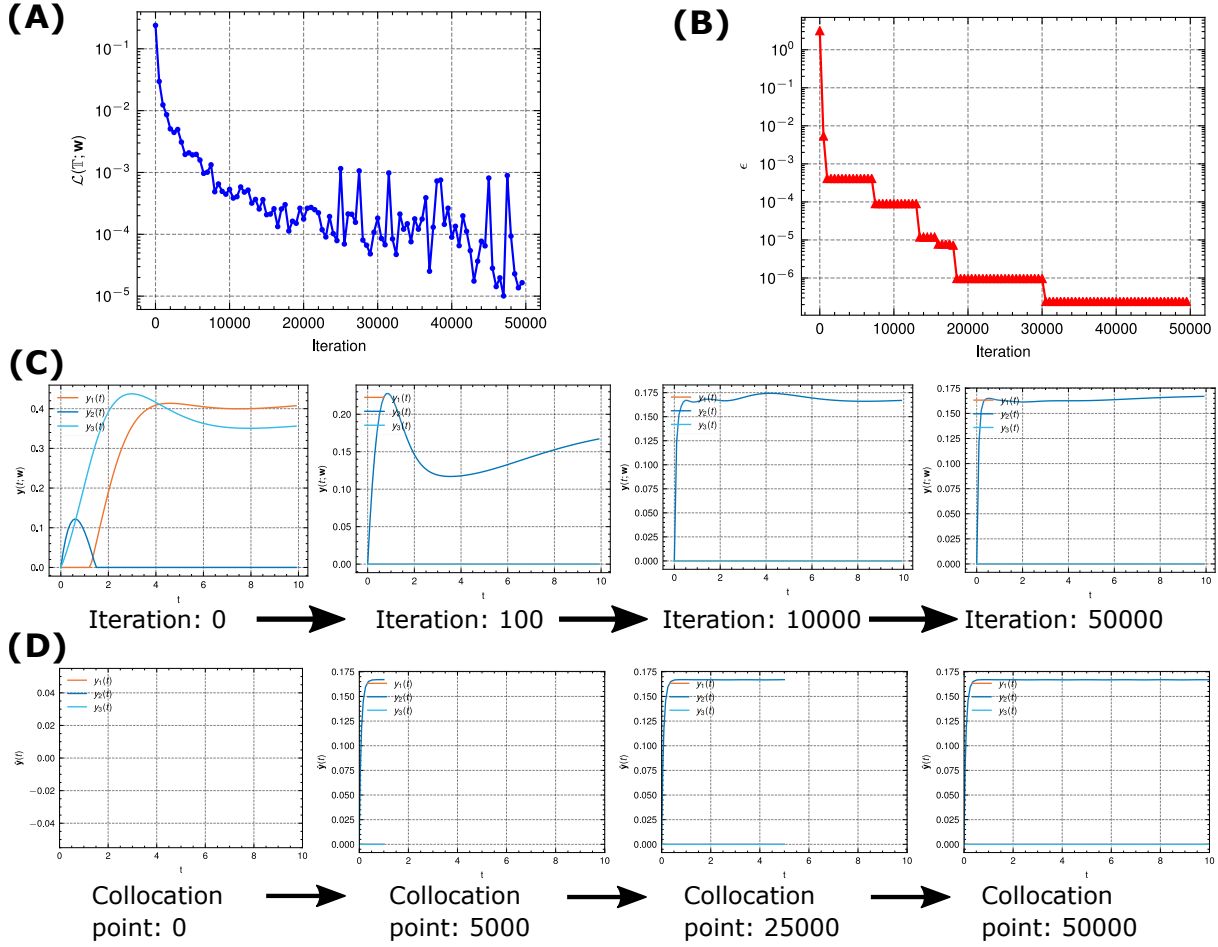


Figure 7: **Example 4** nonlinear complementary problem (A) The loss versus the number of iterations. (B) The epsilon value versus the number of iterations. The epsilon metric is defined in (21) (C) The solving process of the OINN model (D) The solving process of the numerical integration method

Index	OINN		Numerical integration method	
	Iteration	Solution	Collocation point	Solution
Example 4	0	[0.41, 0.00, 0.36]	0	[0.00, 0.00, 0.00]
	10	[0.00, 0.11, 0.00]	10	[0.00, 0.00, 0.00]
	100	[0.00, 0.17, 0.00]	100	[0.00, 0.04, 0.00]
	1000	[0.00, 0.17, 0.00]	1000	[0.00, 0.15, 0.00]
	10000	[0.00, 0.17, 0.00]	10000	[0.00, 0.17, 0.00]
	50000	[0.00, 0.17, 0.00]	50000	[0.00, 0.17, 0.00]

Table 6: **Example 4**, Approximate solutions to the NPE during solving

5.1.5. Convex nonsmooth standard CNLP

Example 5 Consider the following convex nonsmooth standard CNLP

$$\begin{aligned}
 \min_{\mathbf{x}} f(\mathbf{x}) &= 10(x_1 + x_2)^2 + (x_1 - 2)^2 + 20|x_3 - 3| + e^{x_3} \\
 \text{s.t.} & \\
 g(\mathbf{x}) &= (x_1 + 3)^2 + x_2 \leq 36 \\
 h(\mathbf{x}) &= 2x_1 + 5x_3 - 7 = 0.
 \end{aligned} \tag{40}$$

Denote $\mathbf{y} = [x_1, x_2, x_3, u]^T$, where x_1, x_2, x_3 are primal variables, and u is dual variable. Denote $\mathbf{A} = [2, 0, 5]$, $\mathbf{b} = 7$, $\mathbf{U} = \mathbf{A}^T (\mathbf{A}\mathbf{A}^T)^{-1} \mathbf{A}$, and \mathbf{I}_3 is the identity matrix of size 3×3 .

The following ODE system models this CNLP

$$\begin{aligned}
 \frac{d\mathbf{x}}{dt} &= -(\mathbf{I}_3 - \mathbf{U}) (\nabla f(\mathbf{x}) + (u + g(\mathbf{x}))^+ \nabla g(\mathbf{x})) - \mathbf{A}^T h(\mathbf{x}), \\
 \frac{du}{dt} &= \frac{1}{2} (-u + (u + g(\mathbf{x}))^+).
 \end{aligned} \tag{41}$$

The ODE system together with the initial point $\mathbf{y}_0 = [0, 0, 0, 0]$ and time range $[0, 10]$ form the IVP as follow

$$(41), \quad \mathbf{y}_0 = [0, 0, 0, 0], \quad t \in [0, 10] \tag{42}$$

An OINN model, $\mathbf{y}(t; \mathbf{w})$ $t \in [0, 10]$, is built as an approximate state solution to this IVP, and its endpoint $P_{eq}(\mathbf{y}(10; \mathbf{w}))$ is an approximate solution to the CNLP. $P_{eq}(\cdot)$ is a projection function used to project \mathbf{x} onto the equality constraint set $\{\mathbf{x} \in \mathbb{R}^3 \mid h(\mathbf{x}) = 0\}$, as defined in (2).

Index	OINN		Numerical integration method	
	Iteration	Solution	Collocation point	Solution
Example 5	0	[0.51, 0.93, 1.20, 0.00]	0	[0.48, 0.00, 1.21, 0.00]
	10	[-0.30, 0.42, 1.52, 0.34]	10	[0.48, 0.00, 1.21, 0.00]
	100	[-0.87, 0.87, 1.75, 0.00]	100	[0.42, 0.00, 1.23, 0.00]
	1000	[-0.87, 0.87, 1.75, 0.00]	1000	[0.00, 0.07, 1.40, 0.00]
	10000	[-0.86, 0.86, 1.74, 0.00]	10000	[-0.78, 0.77, 1.71, 0.00]
	50000	[-0.86, 0.86, 1.74, 0.00]	50000	[-0.86, 0.86, 1.74, 0.00]

Table 7: **Example 5, Approximate solutions to the CNLP during solving**

Figure 8 shows the training of this OINN model, where the loss decreased from 6.83 to 0.37, and the epsilon value decreased from 62.31 to 39.01. In this example, the epsilon value is defined as the objective value, as in (22). Figure 8 (C) and (D) show the progressions of the approximate state solutions to the IVP (42).

Table 7 displays the progressions of approximate solutions to the CNLP (40). Both the OINN model and

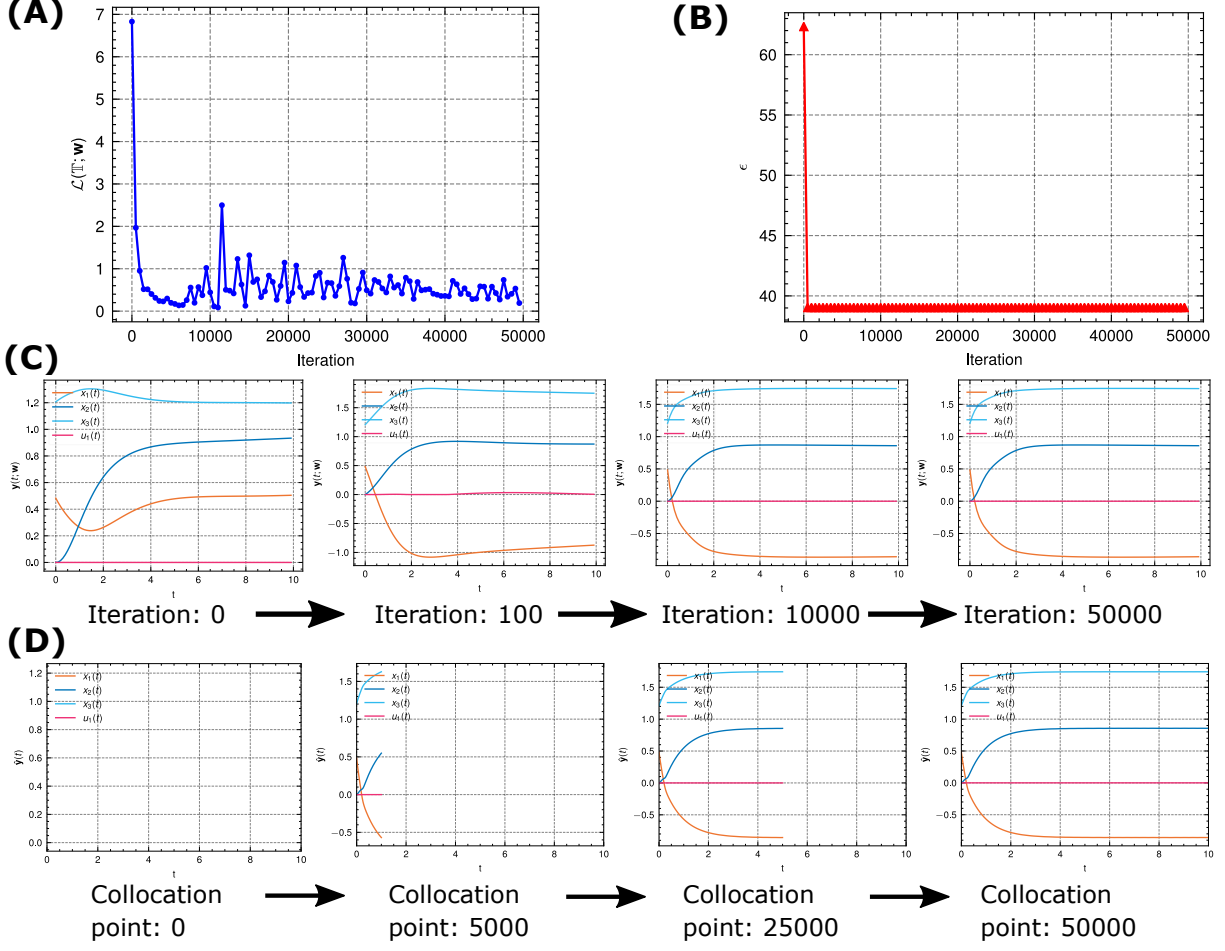


Figure 8: **Example 5** convex nonsmooth standard CNLP (A) The loss versus the number of iterations. (B) The epsilon value versus the number of iterations. The epsilon metric is defined in (22) (C) The solving process of the OINN model (D) The solving process of the numerical integration method

the numerical integration method give the same solution $[-0.86, 0.86, 1.74, 0.00]$, where $[-0.86, 0.86, 1.74]$ is the solution for the primal variable \mathbf{x} , and 0.00 is the solution for the dual variable u .

5.1.6. Pseudoconvex nonsmooth standard CNLP

Example 6 Consider the following pseudoconvex nonsmooth standard CNLP

$$\min_{\mathbf{x}} f(\mathbf{x}) = \frac{x_1 + x_2 + e^{|x_2-1|} - 40}{(x_1 + x_2 + x_3)^2 + 3}$$

s.t.

$$g_1(\mathbf{x}) = -3x_1 + 2x_2 - 5 \leq 0 \tag{43}$$

$$g_2(\mathbf{x}) = x_1^2 + x_2 - 3 \leq 0$$

$$h(\mathbf{x}) = x_1 + 2x_2 + x_3 - 2 = 0$$

Denote $\mathbf{A} = [1, 2, 1]$, $b = 2$, $\mathbf{U} = \mathbf{A}^T (\mathbf{A}\mathbf{A}^T)^{-1} \mathbf{A}$.

The following ODE system model this CNLP

$$\frac{d\mathbf{x}}{dt} = -\theta(t)(\mathbf{I}_3 - \mathbf{U}) (\mu(\mathbf{x})\nabla f(\mathbf{x}) + \partial B(\mathbf{x})) - \text{sign}(h(\mathbf{x}))\mathbf{A}^T, \quad (44)$$

where $\text{sign}(\cdot)$ is the sign function. $\theta(t)$ is defined by

$$\theta(t) = \begin{cases} 0, & \text{if } t \leq T_0 \\ 1, & \text{otherwise,} \end{cases}$$

where $T_0 = 1 + \|\mathbf{A}x_0 - b\|_1 / \lambda_{\min}(\mathbf{A}\mathbf{A}^T)$, $\lambda_{\min}(\mathbf{A}\mathbf{A}^T)$ represents the minimum eigen value of the matrix $\mathbf{A}\mathbf{A}^T$, $\mathbf{x}_0 = [0, 0, 0]$. $\mu(\mathbf{x})$ is defined by

$$\mu(\mathbf{x}) = \begin{cases} 1, & \text{if } g_1(\mathbf{x}) \leq 0 \ \& \ g_2(\mathbf{x}) \leq 0, \\ 0, & \text{otherwise.} \end{cases}$$

$\partial B(\mathbf{x})$ is defined by

$$\partial B(\mathbf{x}) = \begin{cases} 0, & \text{if } g_1(\mathbf{x}) \leq 0 \ \& \ g_2(\mathbf{x}) \leq 0, \\ \nabla g_1(\mathbf{x}), & \text{if } g_1(\mathbf{x}) > 0 \ \& \ g_2(\mathbf{x}) \leq 0, \\ \nabla g_2(\mathbf{x}), & \text{if } g_1(\mathbf{x}) \leq 0 \ \& \ g_2(\mathbf{x}) > 0, \\ \nabla g_1(\mathbf{x}) + \nabla g_2(\mathbf{x}), & \text{if } g_1(\mathbf{x}) > 0 \ \& \ g_2(\mathbf{x}) > 0. \end{cases}$$

The ODE system together with the initial point $\mathbf{y}_0 = [0, 0, 0]$ and time range $[0, 10]$ form the IVP as follow

$$(44), \quad \mathbf{y}_0 = [0, 0, 0], \quad t \in [0, 10] \quad (45)$$

An OINN model, $\mathbf{y}(t; \mathbf{w})$ $t \in [0, 10]$, is built as an approximate state solution for the IVP, and its endpoint $P_{eq}(\mathbf{y}(10; \mathbf{w}))$ is an approximate solution to the CNLP.

Index	OINN		Numerical integration method	
	Iteration	Solution	Collocation point	Solution
Example 6	0	[-0.44, 1.62, -0.81]	0	[0.33, 0.67, 0.33]
	10	[-0.44, 1.62, -0.81]	10	[0.33, 0.67, 0.33]
	100	[-0.56, 1.66, -0.76]	100	[0.33, 0.67, 0.33]
	1000	[-0.52, 1.70, -0.89]	1000	[0.33, 0.67, 0.33]
	10000	[-0.44, 1.84, -1.24]	10000	[-0.63, 1.56, -0.49]
	50000	[-0.44, 1.84, -1.24]	50000	[-0.41, 1.85, -1.28]

Table 8: **Example 6, Approximate solutions to the NPE during solving**

Figure 9 shows the training of the OINN model, where the loss decreased from 1.64 to 1.20, and the epsilon

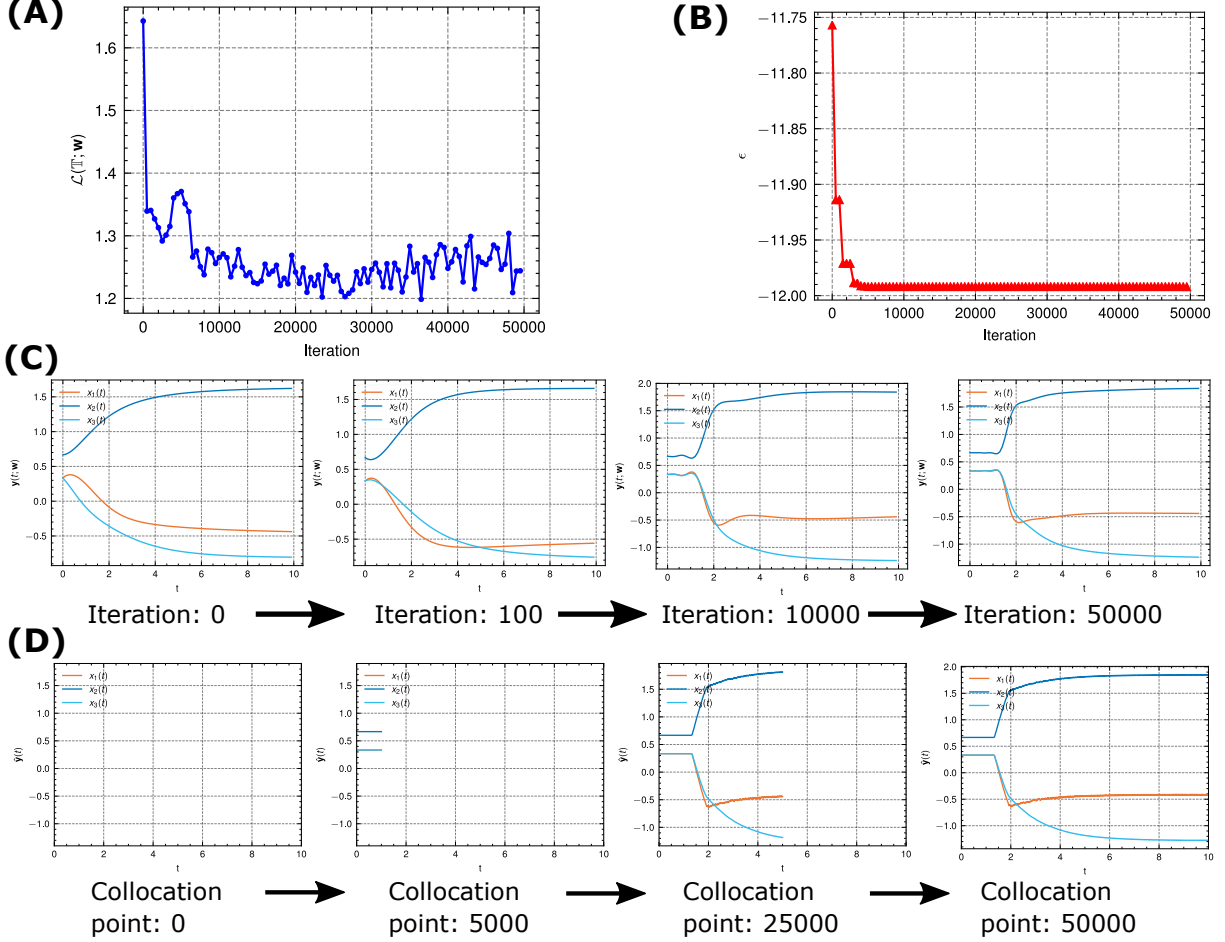


Figure 9: **Example 6 pseudoconvex nonsmooth standard CNLP (A) The loss versus the number of iterations. (B) The epsilon value versus the number of iterations. The epsilon metric is defined in (22) (C) The solving process of the OINN model (D) The solving process of the numerical integration method**

value decreased from -11.75 to -11.99 . Figure 9 (C) and (D) show the progressions of the approximate state solutions to the IVP (45).

Table 8 displays the progressions of the approximate solutions to the CNLP (43). The OINN model gives the final solution of $[-0.44, 1.84, -1.24]$, whereas the numerical integration method give the final solution of $[-0.41, 1.85, -1.28]$.

5.2. Hyperparameters study

In this subsection, we discuss the setting of the two critical hyperparameters in OINN, i.e., initial point and time range. The experiments are based on Example 3 of Section 5.1.3 for illustrative purposes.

Initial point Figure 10 and Table 9 show the convergence behavior of three different initial points. Thanks to the global convergence property of the ODE system, any initial point can converge to the optimal solution, provided there are large enough training iterations. The convergence occurs faster and requires fewer training iterations if the initial point is closer to the optimal solution. For example, the initial point $[20, 0, 0, 8]$ is the closest to the optimal solution $[28.07, -3.00, -3.00, 7.71]$ among the three, so it reaches the

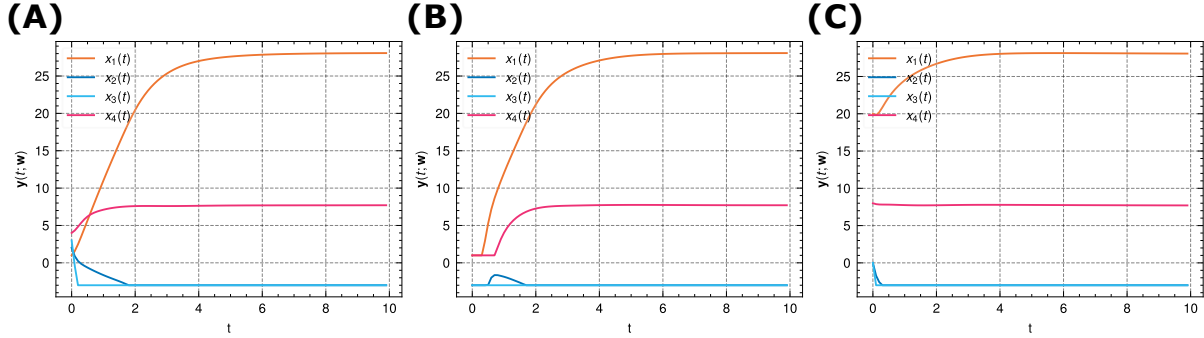


Figure 10: **The OINN models with different initial points (A) Initial point $y_0 = [1, 2, 3, 4]$ (B) Initial point $y_0 = [-10, -15, -10, -14]$ (C) Initial point $y_0 = [20, 0, 0, 8]$**

Time range	Initial point	Iteration	Solution	epsilon ↓
	$y_0 = [1, 2, 3, 4]$	0	[1.46, 2.20, 3.49, 4.21]	6.49
		10	[2.21, 1.46, 2.66, 4.80]	5.66
		100	[2.53, 1.17, 2.32, 4.97]	5.32
		1000	[25.65, -3.00, -3.00, 8.00]	2.42
		10000	[28.07, -3.00, -3.00, 7.71]	0.00
$t \in [0, 10]$	$y_0 = [-10, -15, -10, -14]$	0	[1.00, -3.00, -3.00, 1.00]	28.11
		10	[1.00, -3.00, -3.00, 1.00]	28.11
		100	[1.00, -3.00, -3.00, 1.00]	28.11
		1000	[15.93, -1.35, -3.00, 9.69]	4.04
		10000	[28.07, -3.00, -3.00, 7.71]	0.00
	$y_0 = [20, 0, 0, 8]$	0	[18.92, -0.92, 0.24, 7.53]	3.24
		10	[18.52, -1.58, -0.46, 6.88]	2.54
		100	[18.52, -1.58, -0.46, 6.88]	2.54
		1000	[28.30, -3.00, -3.00, 7.6]	0.23
		10000	[28.07, -3.00, -3.00, 7.71]	0.00

Table 9: **OINN solutions with different initial points**

lowest epsilon value of 0.23 at the 1000th iteration, while the epsilon values of the other two are 2.42 and 4.04.

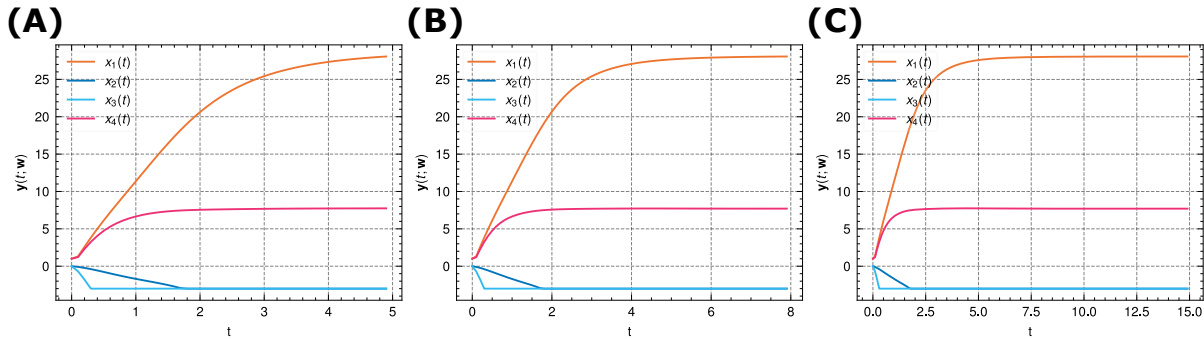


Figure 11: **The OINN models with different time ranges (A) Time range $t \in [0, 5]$ (B) Time range $t \in [0, 8]$ (C) Time range $t \in [0, 15]$**

Time range Figure 11 and Table 10 show the OINN model of the same initial point with different time ranges. The first time range $[0, 5]$ still has an epsilon value of 0.07 after 10,000 iterations. This is because

Initial point	Time range	Iteration	Solution	epsilon ↓
$\mathbf{y}_0 = [0, 0, 0, 0]$	$t \in [0, 5]$	0	[1.00, -0.71, -0.42, 1.00]	16.66
		10	[1.00, -0.59, -1.24, 1.36]	16.08
		100	[3.77, -0.25, -3.00, 5.30]	10.92
		1000	[25.82, -3.00, -3.00, 7.92]	2.26
		10000	[28.11, -3.00, -3.00, 7.74]	0.07
	$t \in [0, 8]$	0	[1.00, 1.47, 2.12, 1.48]	8.08
		10	[1.00, 1.10, 1.74, 1.83]	7.64
		100	[1.00, 1.10, 1.74, 1.83]	7.64
		1000	[26.42, -3.00, -3.00, 8.13]	1.65
		10000	[28.07, -3.00, -3.00, 7.71]	0.00
	$t \in [0, 15]$	0	[1.00, 0.02, -0.13, 1.00]	12.99
		10	[1.00, 0.02, -0.13, 1.00]	12.99
		100	[3.07, 0.15, -3.00, 3.50]	9.69
		1000	[25.98, -3.00, -3.00, 7.76]	2.09
		10000	[28.07, -3.00, -3.00, 7.70]	0.00

Table 10: **OINN solutions with different time ranges**

the OINN model has reached the upper limit of accuracy. The time ranges $[0, 8]$ and $[0, 15]$ both eventually reach an epsilon value of 0.00. The time range $[0, 8]$ converges faster than the time range $[0, 15]$ because the former has a smaller span and is easier to train than the latter.

5.3. Discussions

The OINN method and numerical integration methods solve CNLP in different ways and are based on different software implementations. Because of that, it is difficult to determine which method is superior to the other. In this subsection, we first highlight some of OINN’s computational advantages and then discuss its limitations.

Index	OINN		Numerical integration method	
	Iteration	Epsilon: NPE error ↓	Collocation point	Epsilon: NPE error ↓
Example 3	0	10.925	0	13.111
	10	10.925	10	13.123
	100	10.925	100	13.223
	1000	1.550	1000	12.093
	10000	0.001	10000	7.307
	50000	0.001	50000	0.006
Example 4	0	3.117	0	2.437
	10	0.738	10	2.350
	100	0.007	100	1.728
	1000	0.000	1000	0.160
	10000	0.000	10000	0.001
	50000	0.000	50000	0.001

Table 11: **Comparison of solutions accuracy** The epsilon metric is defined in (21).

Tables 11 and 12 display the epsilon values while Examples 3-6 were being resolved, where the OINN model converges with training iterations and the numerical integration method converges as the collocation point progresses. In Examples 3 and 4, the OINN model reaches a lower final epsilon error than the numerical

Index	OINN		Numerical integration method	
	Iteration	Epsilon: Objective value ↓	Collocation point	Epsilon: Objective value ↓
Example 5	0	62.315	0	43.838
	10	39.633	10	43.757
	100	39.020	100	43.130
	1000	39.020	1000	40.120
	10000	39.020	10000	39.029
	50000	39.020	50000	39.020
Example 6	0	-11.757	0	-7.871
	10	-11.757	10	-7.871
	100	-11.861	100	-7.871
	1000	-11.914	1000	-7.871
	10000	-11.992	10000	inf
	50000	-11.992	50000	-11.985

Table 12: **Comparison of objective values** The epsilon metric is defined in (22). inf means that the solution is not feasible.

integration method, indicating that OINN found a better solution to satisfy the CNLPs. In Example 6, the OINN model reaches a lower objective value of -11.992 , while the numerical integration method only manages to reach the objective value of -11.985 .

OINN can give an approximate solution to the CNLP at any round of iterations, while the numerical integration method can only give the solution at the end of the program. Thanks to that, OINN can provide more accurate approximate solutions in the early stage of the solving process. For instance, in Example 3, the OINN’s epsilon error has decreased to 1.55 by the 1000th training iteration, compared to 12.093 of the numerical integration method.

Index	OINN		Numerical integration methods						
	Iteration	CPU time	Collocation point	RK45 CPU time	RK23 CPU time	DOP853 CPU time	Radau CPU time	BDF CPU time	LSODA CPU time
Example 6	10	202 ms	10	1350 ms	860 ms	3470 ms	1000 ms	Fail	157 ms
	100	893 ms	100	1740 ms	1090 ms	4620 ms	1330 ms	Fail	154 ms
	1000	8.47 s	1000	2.14s	1.32s	5.68 s	1.47 s	Fail	188 ms
	10000	1min 20s	10000	1min 25s	5min 5s	34min 29s	Fail	Fail	4h 4min 35s
	50000	7min 55s	50000	14min 29s	25min 14s	1h 43min 28s	Fail	Fail	Fail

Table 13: **CPU times of the OINN method and numerical integration methods.** RK45, RK23, DOP853, Radau, BDF and LSODA are six different numerical integration methods. ms, s, min, and h refer to milliseconds, seconds, minutes, and hours respectively.

Table 13 shows the CPU times for solving Example 6, which has a stiff ODE system and is challenging to solve numerically. We compare OINN with six different numerical integration methods. OINN outperforms all these six methods in terms of computational CPU time, i.e., OINN takes 7min 55s while RK45 takes at best 14min 29s. The three methods, Radau, BDF, and LSODA, fail to solve this problem.

We must emphasize that the proposed OINN should not be seen as a substitute for the conventional numerical integration methods. Such methods have been developed for many years and are well known to meet the requirements of reliability. OINN research is still in its early stages, making it difficult to go beyond traditional methods for many practical problems. Our contribution is to open up a fresh perspective and a

new line of research to solve CNLP.

6. Conclusion

We propose a deep learning approach to address CNLPs, namely OINN. We give a complete description of solving CNLPs by OINN, including neurodynamic optimization approaches, the OINN framework, and the training algorithm. By doing so, we connect this longstanding problem with deep learning and machine learning communities. With the rapid development of deep learning research, both methodologically and experimentally, we believe that this work will lead to ongoing contributions that can benefit a wide range of practitioners in optimization.

There are many possible future directions for this work; we give some examples here. 1) How to design a better neural network structure and activation function for the OINN model? 2) What is the difference terms of computational effort and quality of the solution when using various epsilon metrics for the same CNLP? 3) How to design appropriate epsilon metrics for other CNLPs? We can gradually make our proposed approach more robust by providing answers to these questions.

Bibliography

- Anitescu, C., Atroshchenko, E., Alajlan, N., & Rabczuk, T. (2019). Artificial neural network methods for the solution of second order boundary value problems. *Computers, Materials and Continua*, 59, 345–359.
- Baydin, A. G., Pearlmutter, B. A., Radul, A. A., & Siskind, J. M. (2018). Automatic differentiation in machine learning: a survey. *Journal of machine learning research*, 18.
- Beck, C., Jentzen, A. et al. (2019). Machine learning approximation algorithms for high-dimensional fully nonlinear partial differential equations and second-order backward stochastic differential equations. *Journal of Nonlinear Science*, 29, 1563–1619.
- Bertsekas, D. P. (1997). Nonlinear programming. *Journal of the Operational Research Society*, 48, 334–334.
- Bogacki, P., & Shampine, L. F. (1989). A 3 (2) pair of runge-kutta formulas. *Applied Mathematics Letters*, 2, 321–325.
- Boyd, S., Boyd, S. P., & Vandenberghe, L. (2004). *Convex optimization*. Cambridge university press.
- Bradbury, J., Frostig, R., Hawkins, P., Johnson, M. J., Leary, C., Maclaurin, D., Necula, G., Paszke, A., VanderPlas, J., Wanderman-Milne, S., & Zhang, Q. (2018). JAX: composable transformations of Python+NumPy programs. URL: <http://github.com/google/jax>.
- Butcher, J. C. (2016). *Numerical methods for ordinary differential equations*. John Wiley & Sons.

- Cappart, Q., Chételat, D., Khalil, E., Lodi, A., Morris, C., & Veličković, P. (2021). Combinatorial optimization and reasoning with graph neural networks. *arXiv preprint arXiv:2102.09544*, .
- Chen, F., Sondak, D., Protopapas, P., Mattheakis, M., Liu, S., Agarwal, D., & Giovanni, M. D. (2020). Neurodiffq: A python package for solving differential equations with neural networks. *Journal of Open Source Software*, 5, 1931. URL: <https://doi.org/10.21105/joss.01931>. doi:10.21105/joss.01931.
- Cybenko, G. (1989). Approximation by superpositions of a sigmoidal function. *Mathematics of Control, Signals and Systems*, 2, 303–314. URL: <https://doi.org/10.1007/BF02551274>. doi:10.1007/BF02551274.
- Devlin, J., Chang, M., Lee, K., & Toutanova, K. (2018). BERT: pre-training of deep bidirectional transformers for language understanding. *CoRR*, *abs/1810.04805*. URL: <http://arxiv.org/abs/1810.04805>. arXiv:1810.04805.
- Dissanayake, M. W. M. G., & Phan-Thien, N. (1994). Neural-network-based approximations for solving partial differential equations. *Communications in Numerical Methods in Engineering*, 10, 195–201. URL: <https://onlinelibrary.wiley.com/doi/abs/10.1002/cnm.1640100303>. doi:<https://doi.org/10.1002/cnm.1640100303>. arXiv:<https://onlinelibrary.wiley.com/doi/pdf/10.1002/cnm.1640100303>.
- Dormand, J. R., & Prince, P. J. (1980). A family of embedded runge-kutta formulae. *Journal of computational and applied mathematics*, 6, 19–26.
- Flamant, C., Protopapas, P., & Sondak, D. (2020). Solving differential equations using neural network solution bundles. arXiv:2006.14372.
- Forti, M., Nistri, P., & Quincampoix, M. (2004). Generalized neural network for nonsmooth nonlinear programming problems. *IEEE Transactions on Circuits and Systems I: Regular Papers*, 51, 1741–1754.
- Gao, X.-B., Liao, L.-Z., & Xue, W. (2004). A neural network for a class of convex quadratic minimax problems with constraints. *IEEE transactions on neural networks*, 15, 622–628.
- Goodfellow, I., Bengio, Y., & Courville, A. (2016). *Deep Learning*. MIT Press. <http://www.deeplearningbook.org>.
- Guo, H., Zhuang, X., & Rabczuk, T. (2021). A deep collocation method for the bending analysis of kirchhoff plate. *arXiv preprint arXiv:2102.02617*, .
- Guo, Z., Liu, Q., & Wang, J. (2011). A one-layer recurrent neural network for pseudoconvex optimization subject to linear equality constraints. *IEEE Transactions on Neural Networks*, 22, 1892–1900.
- Hairer, E., Nørsett, S. P., & Wanner, G. (1993). *Solving ordinary differential equations. 1, Nonstiff problems*. Springer-Vlg.

- Han, J., Jentzen, A., & E, W. (2018). Solving high-dimensional partial differential equations using deep learning. *Proceedings of the National Academy of Sciences*, *115*, 8505–8510.
- Han, J., Jentzen, A. et al. (2017). Deep learning-based numerical methods for high-dimensional parabolic partial differential equations and backward stochastic differential equations. *Communications in mathematics and statistics*, *5*, 349–380.
- Harker, P. T., & Pang, J.-S. (1990). Finite-dimensional variational inequality and nonlinear complementarity problems: a survey of theory, algorithms and applications. *Mathematical programming*, *48*, 161–220.
- Hopfield, J. J., & Tank, D. W. (1985). “neural” computation of decisions in optimization problems. *Biological cybernetics*, *52*, 141–152.
- Hornik, K., Stinchcombe, M., & White, H. (1989). Multilayer feedforward networks are universal approximators. *Neural Networks*, *2*, 359–366. URL: <https://www.sciencedirect.com/science/article/pii/0893608089900208>. doi:[https://doi.org/10.1016/0893-6080\(89\)90020-8](https://doi.org/10.1016/0893-6080(89)90020-8).
- Jumper, J., Evans, R., Pritzel, A., Green, T., Figurnov, M., Ronneberger, O., Tunyasuvunakool, K., Bates, R., Žídek, A., Potapenko, A. et al. (2021). Highly accurate protein structure prediction with alphafold. *Nature*, *596*, 583–589.
- Kennedy, M. P., & Chua, L. O. (1988). Neural networks for nonlinear programming. *IEEE Transactions on Circuits and Systems*, *35*, 554–562.
- Krizhevsky, A., Sutskever, I., & Hinton, G. E. (2012). Imagenet classification with deep convolutional neural networks. *Advances in neural information processing systems*, *25*, 1097–1105.
- Lagaris, I., Likas, A., & Fotiadis, D. (1998). Artificial neural networks for solving ordinary and partial differential equations. *IEEE Transactions on Neural Networks*, *9*, 987–1000. doi:10.1109/72.712178.
- Lagaris, I. E., Likas, A. C., & Papageorgiou, D. G. (2000). Neural-network methods for boundary value problems with irregular boundaries. *IEEE Transactions on Neural Networks*, *11*, 1041–1049.
- Leung, M.-F., & Wang, J. (2020). Minimax and biobjective portfolio selection based on collaborative neurodynamic optimization. *IEEE transactions on neural networks and learning systems*, *32*, 2825–2836.
- Lu, L., Meng, X., Mao, Z., & Karniadakis, G. E. (2021). Deepxde: A deep learning library for solving differential equations. *SIAM Review*, *63*, 208–228. URL: <http://dx.doi.org/10.1137/19M1274067>. doi:10.1137/19m1274067.
- Mattheakis, M., Sondak, D., Dogra, A. S., & Protopapas, P. (2022). Hamiltonian neural networks for solving equations of motion. *Physical Review E*, *105*, 065305.

- McFall, K. S., & Mahan, J. R. (2009). Artificial neural network method for solution of boundary value problems with exact satisfaction of arbitrary boundary conditions. *IEEE Transactions on Neural Networks*, *20*, 1221–1233.
- Min, S., Lee, B., & Yoon, S. (2017). Deep learning in bioinformatics. *Briefings in bioinformatics*, *18*, 851–869.
- Nair, V., Bartunov, S., Gimeno, F., von Glehn, I., Lichocki, P., Lobov, I., O’Donoghue, B., Sonnerat, N., Tjandraatmadja, C., Wang, P. et al. (2020). Solving mixed integer programs using neural networks. *arXiv preprint arXiv:2012.13349*, .
- Parise, F., & Ozdaglar, A. (2019). A variational inequality framework for network games: Existence, uniqueness, convergence and sensitivity analysis. *Games and Economic Behavior*, *114*, 47–82.
- Paszke, A., Gross, S., Massa, F., Lerer, A., Bradbury, J., Chanan, G., Killeen, T., Lin, Z., Gimelshein, N., Antiga, L., Desmaison, A., Kopf, A., Yang, E., DeVito, Z., Raison, M., Tejani, A., Chilamkurthy, S., Steiner, B., Fang, L., Bai, J., & Chintala, S. (2019). Pytorch: An imperative style, high-performance deep learning library. In *Advances in Neural Information Processing Systems 32* (pp. 8024–8035). Curran Associates, Inc. URL: <http://papers.neurips.cc/paper/9015-pytorch-an-imperative-style-high-performance-deep-learning-library.pdf>.
- Patriksson, M. (2013). *Nonlinear programming and variational inequality problems: a unified approach* volume 23. Springer Science & Business Media.
- Petzold, L. (1983). Automatic selection of methods for solving stiff and nonstiff systems of ordinary differential equations. *SIAM journal on scientific and statistical computing*, *4*, 136–148.
- Qin, S., Bian, W., & Xue, X. (2013). A new one-layer recurrent neural network for nonsmooth pseudoconvex optimization. *Neurocomputing*, *120*, 655–662.
- Qin, S., & Xue, X. (2014). A two-layer recurrent neural network for nonsmooth convex optimization problems. *IEEE transactions on neural networks and learning systems*, *26*, 1149–1160.
- Raissi, M., Perdikaris, P., & Karniadakis, G. (2019). Physics-informed neural networks: A deep learning framework for solving forward and inverse problems involving nonlinear partial differential equations. *Journal of Computational Physics*, *378*, 686–707. URL: <https://www.sciencedirect.com/science/article/pii/S0021999118307125>. doi:<https://doi.org/10.1016/j.jcp.2018.10.045>.
- Robinson, S. M. (1992). Normal maps induced by linear transformations. *Mathematics of Operations Research*, *17*, 691–714.
- Rodriguez-Vazquez, A., Dominguez-Castro, R., Rueda, A., Huertas, J. L., & Sanchez-Sinencio, E. (1990). Nonlinear switched capacitor’neural’networks for optimization problems. *IEEE Transactions on Circuits and Systems*, *37*, 384–398.

- Samaniego, E., Anitescu, C., Goswami, S., Nguyen-Thanh, V. M., Guo, H., Hamdia, K., Zhuang, X., & Rabczuk, T. (2020). An energy approach to the solution of partial differential equations in computational mechanics via machine learning: Concepts, implementation and applications. *Computer Methods in Applied Mechanics and Engineering*, *362*, 112790.
- Shampine, L. F., & Reichelt, M. W. (1997). The matlab ode suite. *SIAM journal on scientific computing*, *18*, 1–22.
- Singh, V. V., & Lisser, A. (2018). Variational inequality formulation for the games with random payoffs. *Journal of Global Optimization*, *72*, 743–760.
- Sirignano, J., & Spiliopoulos, K. (2018). Dgm: A deep learning algorithm for solving partial differential equations. *Journal of computational physics*, *375*, 1339–1364.
- Sonoda, S., & Murata, N. (2017). Neural network with unbounded activation functions is universal approximator. *Applied and Computational Harmonic Analysis*, *43*, 233–268. URL: <https://www.sciencedirect.com/science/article/pii/S1063520315001748>. doi:<https://doi.org/10.1016/j.acha.2015.12.005>.
- Virtanen, P., Gommers, R., Oliphant, T. E., Haberland, M., Reddy, T., Cournapeau, D., Burovski, E., Peterson, P., Weckesser, W., Bright, J., van der Walt, S. J., Brett, M., Wilson, J., Millman, K. J., Mayorov, N., Nelson, A. R. J., Jones, E., Kern, R., Larson, E., Carey, C. J., Polat, İ., Feng, Y., Moore, E. W., VanderPlas, J., Laxalde, D., Perktold, J., Cimrman, R., Henriksen, I., Quintero, E. A., Harris, C. R., Archibald, A. M., Ribeiro, A. H., Pedregosa, F., van Mulbregt, P., & SciPy 1.0 Contributors (2020). SciPy 1.0: Fundamental Algorithms for Scientific Computing in Python. *Nature Methods*, *17*, 261–272. doi:10.1038/s41592-019-0686-2.
- Wang, Y., Li, X., & Wang, J. (2021). A neurodynamic optimization approach to supervised feature selection via fractional programming. *Neural Networks*, *136*, 194–206.
- Wanner, G., & Hairer, E. (1996). *Solving ordinary differential equations II* volume 375. Springer Berlin Heidelberg New York.
- Wu, D., & Lisser, A. (2022). A dynamical neural network approach for solving stochastic two-player zero-sum games. *Neural Networks*, .
- Xia, Y., & Feng, G. (2007). A new neural network for solving nonlinear projection equations. *Neural Networks*, *20*, 577–589.
- Xia, Y., Leung, H., & Wang, J. (2002). A projection neural network and its application to constrained optimization problems. *IEEE Transactions on Circuits and Systems I: Fundamental Theory and Applications*, *49*, 447–458.

- Xia, Y., & Wang, J. (2015). A bi-projection neural network for solving constrained quadratic optimization problems. *IEEE transactions on neural networks and learning systems*, *27*, 214–224.
- Xiao, L., & Boyd, S. (2006). Optimal scaling of a gradient method for distributed resource allocation. *Journal of optimization theory and applications*, *129*, 469–488.
- Xu, C., Chai, Y., Qin, S., Wang, Z., & Feng, J. (2020). A neurodynamic approach to nonsmooth constrained pseudoconvex optimization problem. *Neural Networks*, *124*, 180–192.
- Xue, X., & Bian, W. (2008). Subgradient-based neural networks for nonsmooth convex optimization problems. *IEEE Transactions on Circuits and Systems I: Regular Papers*, *55*, 2378–2391.
- Yu, B. et al. (2018). The deep ritz method: a deep learning-based numerical algorithm for solving variational problems. *Communications in Mathematics and Statistics*, *6*, 1–12.